nature cell biology

Per2 induction limits lymphoid-biased haematopoietic stem cells and lymphopoiesis in the context of DNA damage and ageing

Jianwei Wang[1,5], Yohei Morita[1], Bing Han[1], Silke Niemann[2], Bettina Löffler[3] and K. Lenhard Rudolph[1,4,6]

Ageing-associated impairments in haemato-lymphopoiesis are associated with DNA damage accumulation and reduced maintenance of lymphoid-biased (Ly-biased) compared with myeloid-biased (My-biased) haematopoietic stem cells (HSCs). Here, *in vivo* RNAi screening identifies period circadian clock 2 (*Per2*) as a critical factor limiting the maintenance of HSCs in response to DNA damage and ageing. Under these conditions, *Per2* is activated predominantly in Ly-biased HSCs and stimulates DNA damage signalling and p53-dependent apoptosis in haematopoietic cells. *Per2* deletion ameliorates replication stress and DNA damage responses in haematopoietic cells, thereby improving the maintenance of Ly-biased HSCs, lymphopoiesis, and immune function in ageing mice without increasing the accumulation of DNA damage. *Per2*-deficient mice retain *Batf/p53*-dependent induction of differentiation of HSCs in response to DNA damage and exhibit an elongated lifespan. Together, these results identify *Per2* as a negative regulator of Ly-biased HSCs and immune functions in response to DNA damage and ageing.

The function of haematopoietic stem cells (HSCs) declines during ageing in both mice and men[1–4]. In particular, the lymphopoietic potential of HSCs strongly diminishes during ageing and this decline is thought to contribute to the evolution of immune defects limiting overall fitness and organismal survival during ageing[5–7]. Studies on laboratory mice revealed that the HSC pool consists of functionally distinct subpopulations of HSCs including lymphoid-biased HSCs (Ly-biased HSCs) preferentially differentiating into the lymphoid lineage and myeloid-biased HSCs (My-biased HSCs) preferentially differentiating into the myeloid lineage[8,9]. During ageing, there is a decline in Ly-biased HSCs relative to the number of My-biased HSCs, which is thought to contribute to the ageing-associated decrease in lymphopoiesis and the relative dominance of myelopoiesis in both mice and men[10]. The molecular causes for this ageing-associated drift in the HSC pool are yet to be delineated.

There is experimental evidence that the accumulation of DNA damage contributes to ageing-induced impairments in haemato-/lymphopoiesis[11,12]. Different factors could contribute to the ageing-associated accumulation of DNA damage in HSCs, including oxidative stress[13,14], DNA replication stress[15], oxidative stress in response to proliferation[16], and telomere shortening, which is associated with bone marrow failure, and myelodysplastic syndromes in ageing humans[17–21].

Here, we conducted an *in vivo* RNA-mediated interference (RNAi) screen targeting 459 putative tumour suppressor genes to identify hitherto uncharacterized checkpoint responses limiting the self-renewal and functional reserve of HSCs in response to DNA damage. The current study provides experimental evidence that the upregulation of *Per2* contributes to the induction of DNA damage responses in haematopoietic stem and progenitor cells and to the selective vulnerability of Ly-biased HSCs to DNA damage and ageing.

RESULTS

Stable RNAi screening identifies period circadian gene 2 (*Per2*) as a checkpoint component limiting the maintenance of haematopoietic stem cells in response to telomere dysfunction

Homozygous telomerase knockout mice ($mTerc^{-/-}$) lack telomerase activity but the first generation of knockout mice (G1 $mTerc^{-/-}$) does not show significant ageing phenotypes owing to long telomere reserves[22,23]. When bred through successive generations on a C57BL/6J background, third-generation knockout mice (G3 $mTerc^{-/-}$) exhibit critically short, dysfunctional telomeres resulting

[1]Research Group on Stem Cell Aging, Leibniz Institute on Aging – Fritz Lipmann Institute (FLI), Beutenbergstr. 11, 07745 Jena, Germany. [2]Institute for Medical Microbiology, University Hospital Münster, Domagkstraße 10, 48149 Münster, Germany. [3]Institute of Medical Microbiology, Jena University Hospital (UKJ), 07747 Jena, Germany. [4]Research Group on Molecular Aging, Faculty of Medicine, Friedrich-Schiller-University, 07745 Jena, Germany. [5]Present address: Institute for Stem Cell Biology and Regenerative Medicine, Tsinghua University, Beijing 100084, China.
[6]Correspondence should be addressed to K.L.R. (e-mail: Lenhard.Rudolph@Leibniz-FLI.de)

Received 11 March 2015; accepted 14 March 2016; published online 18 April 2016; DOI: 10.1038/ncb3342

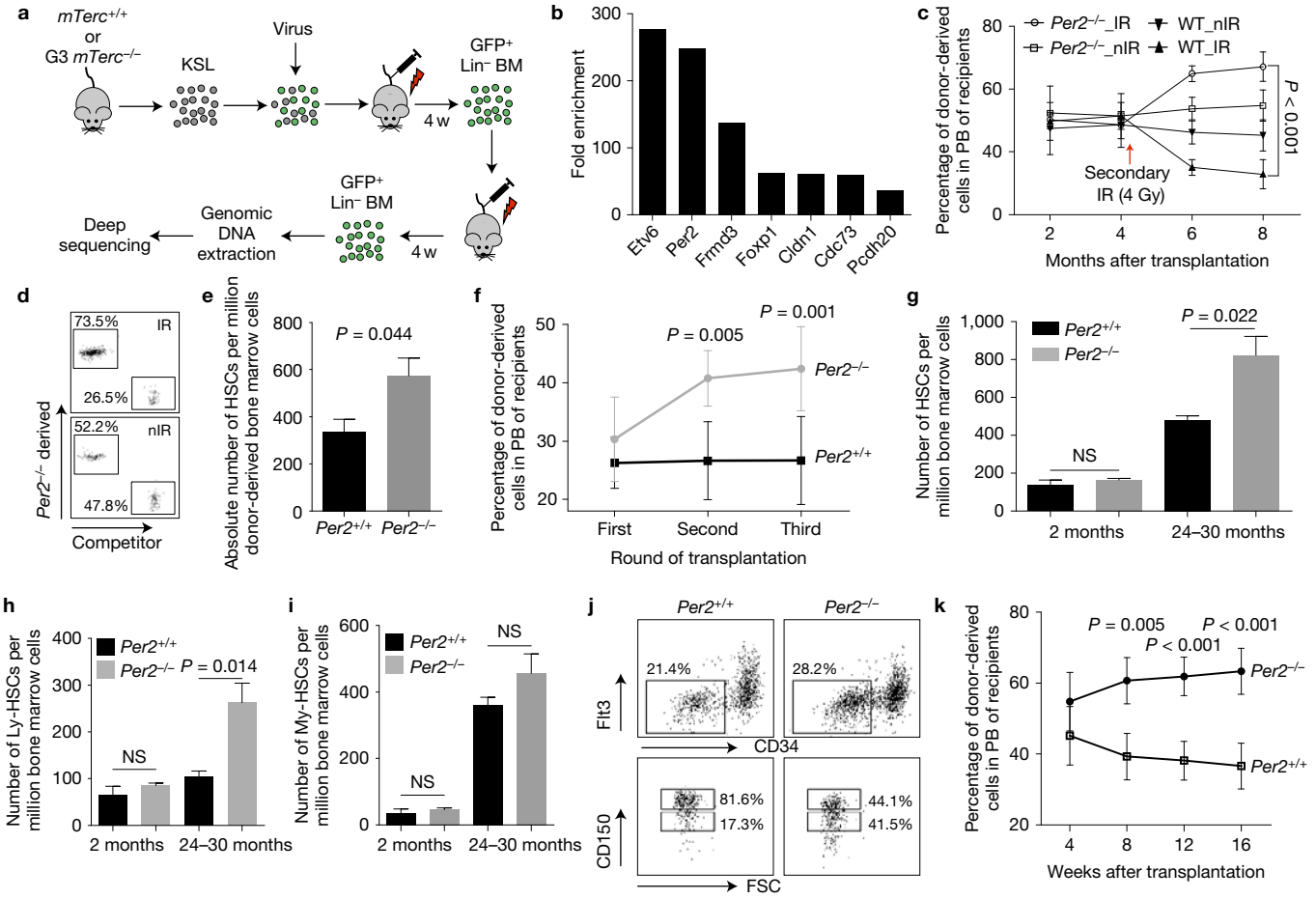

Figure 1 *Per2* deletion improves self-renewal and function of HSCs in response to telomere shortening, γ-irradiation, replication stress and physiological ageing. (**a**) Scheme of the *in vivo* screen using transplanted haematopoietic stem and progenitor (KSL) cells from 3-month-old *mTerc*$^{+/+}$ and G3 *mTerc*$^{-/-}$ mice that were infected with a lentiviral pool of shRNAs targeting 459 putative tumour suppressor genes (see Methods). (**b**) Positively selected shRNAs in Lin$^-$ cells derived from G3 *mTerc*$^{-/-}$ compared with *mTerc*$^{+/+}$ donors (see also Supplementary Fig. 1A–E and Supplementary Table 1). (**c**–**e**) Competitive transplantation of 100 freshly isolated HSCs (CD34$^-$ KSL) from 2-month-old *Per2*$^{-/-}$ or *Per2*$^{+/+}$ mice along with total bone marrow competitor cells into lethally irradiated recipients. After stable engraftment (4 months), half of the recipients received a second dose of sub-lethal irradiation (IR, 4 Gy). (**c**) Peripheral blood (PB) chimaerism at the indicated time points after transplantation with or without secondary IR at 4 months. (**d**) Representative FACS plots on chimaerism of *Per2*$^{-/-}$ donor-derived cells and competitor cells in peripheral blood. Upper panel, 4 months after second IR; lower panel, the same time point without the second IR (nIR). (**e**) Absolute number of *Per2*$^{-/-}$ or *Per2*$^{+/+}$ donor-derived HSCs (CD34$^-$ KSL) in bone marrow, 4 months after the second IR. (**f**) Serial, competitive transplantation of 10^6 total bone marrow cells of 2-month-old *Per2*$^{-/-}$ or *Per2*$^{+/+}$ mice for three rounds into lethally irradiated recipients (see Methods). Chimaerism of test donor-derived cells in peripheral blood at the 3-month time point in the indicated rounds of transplantation. (**g**–**j**) The number of total HSCs (CD34$^-$ KSL) (**g**), Ly-biased HSCs (CD150^{lo}) (**h**) and My-biased HSCs (CD150^{hi}) (**i**) was determined in bone marrow from 2- and 24–30-month-old, non-transplanted mice of the indicated genotypes. (**j**) Representative FACS plots depicting the composition of My-biased and Ly-biased HSCs in the CD34$^-$ KSL population of 30-month-old *Per2*$^{-/-}$ and *Per2*$^{+/+}$ mice (see also Supplementary Fig. 2A–C). (**k**) Competitive transplantation of 100 HSCs from 20-month-old *Per2*$^{-/-}$ or *Per2*$^{+/+}$ mice into sub-lethally (8 Gy) irradiated recipients. Chimaerism of donor-derived cells in peripheral blood at the indicated time points. (**c**–**f**,**k**) $N = 5$ mice per group; values are shown as mean ± s.e.m.; multiple *t*-test was used to calculate *P* values. (**g**–**i**) $N = 7$ old mice and $N = 10$ young mice; values are shown as mean ± s.e.m.; multiple *t*-test was used to calculate *P* values. NS, not significant.

in premature ageing of organ systems with high rates of cell turnover including the haematopoietic system[17,24]. The activation of DNA damage checkpoints in response to telomere dysfunction limits the self-renewal and the functional reserve of HSCs and other stem cells such as germline stem cells[17,18,25]. A lentiviral short hairpin RNA (shRNA) library targeting putative tumour suppressor genes (Supplementary Table 1) was infected into freshly isolated haematopoietic stem and progenitor cells (c-Kit$^+$, Sca-1$^+$, lineage$^-$ (KSL cells)) from G3 *mTerc*$^{-/-}$ and *mTerc*$^{+/+}$ mice (Fig. 1a). Infected KSL cells were transplanted along with non-infected KSL cells for two rounds into lethally irradiated wild-type recipient mice (Fig. 1a). Deep sequencing analysis of donor-derived haematopoietic cells (lineage marker negative (Lin$^-$)) after two rounds of transplantation identified several shRNAs that were strongly enriched in the cohort transplanted with KSL cells from G3 *mTerc*$^{-/-}$ mice compared with the cohort transplanted with KSL cells from *mTerc*$^{+/+}$ mice (Fig. 1b), suggesting that these shRNA-targeted genes limit the maintenance of HSCs in response to telomere shortening. Indeed,

transplantation experiments with single-shRNA-targeted KSL cells confirmed two candidate genes (*Per2* and *Pcdh20*) that rescued the repopulation capacity of telomere-dysfunctional haematopoietic cells from G3 *mTerc*$^{-/-}$ mice compared with haematopoietic cells with long telomeres from *mTerc*$^{+/+}$ mice (Supplementary Fig. 1A–E). *Per2* knockdown also showed a mild positive selection in mice transplanted with lentivirus-targeted KSL cells from *mTerc*$^{+/+}$ donor mice, but the positive selection was more pronounced in KSL cells from G3 *mTerc*$^{-/-}$ mice (Supplementary Fig. 1D).

Homozygous deletion of *Per2* improves HSC maintenance and function in the context of irradiation, replicative stress and ageing

To test whether the *Per2* gene status would affect the maintenance of HSCs in the context of different types of DNA damage, HSCs from homozygous *Per2* knockout (*Per2*$^{-/-}$) mice[26] were analysed in comparison with *Per2*$^{+/+}$ mice.

First, 100 purified HSCs (CD34^{-} KSL) from either 2-month-old *Per2*$^{-/-}$ or *Per2*$^{+/+}$ mice (both CD45.2) were transplanted along with 1 million competitor cells (total bone marrow from 2-month-old CD45.1 mice) into lethally irradiated recipients ($n = 10$ per group). Four months after transplantation, five mice per group received a second dose (4 Gy) of sub-lethal γ-irradiation and changes in the chimaerism of peripheral blood cells were determined at 2-month intervals. This analysis revealed a significant positive selection of *Per2*$^{-/-}$ haematopoiesis compared with *Per2*$^{+/+}$ haematopoiesis in response to γ-irradiation ($P < 0.001$) both in peripheral blood cells (Fig. 1c,d) and at the level of HSCs (CD34^{-} KSL) (Fig. 1e).

Second, DNA replication stress represents another type of DNA damage, which limits the self-renewal of HSCs during ageing and serial transplantation[15,16,27]. To determine the possible influence of *Per2* gene status, 1 million total bone marrow cells from 2-month-old *Per2*$^{-/-}$ donor mice or age-matched *Per2*$^{+/+}$ donor mice (both CD45.2) were serially transplanted along with 2 million competitor cells (total bone marrow cells from CD45.1 mice) into lethally irradiated CD45.1/CD45.2 recipients. Analysis of peripheral blood chimaerism revealed a significant positive selection of *Per2*$^{-/-}$ haematopoiesis compared with *Per2*$^{+/+}$ haematopoiesis in the second ($P = 0.005$) and third round ($P = 0.001$) of transplantation (Fig. 1f). Of note, the numbers of HSCs in 2-month-old donor mice were not affected by *Per2* gene status (Fig. 1g–j), indicating that serial transplantation reflected declines in the functional capacity of HSCs in the above-described serial transplantation experiments.

Third, to determine the influence of *Per2* gene status on the function of physiologically aged HSCs, 100 freshly isolated HSCs of 20-month-old Per2$^{-/-}$ mice (CD45.2) were transplanted into sub-lethally irradiated recipients (CD45.1/CD45.2) together with 100 HSCs of age-matched *Per2*$^{+/+}$ mice (CD45.1). Analysis of peripheral blood chimaerism revealed a significantly improved reconstitution capacity of HSCs from aged *Per2*$^{-/-}$ mice compared with HSCs from *Per2*$^{+/+}$ mice in long-term engrafted, primary recipients (Fig. 1k).

Together, these data indicated that *Per2* deletion enhances the maintenance and repopulation capacity of HSCs in the context of DNA damage, replication stress and ageing. To determine the influence of *Per2* gene status on the maintenance of endogenous, non-transplanted HSCs during ageing, cohorts of 24–30-month-old *Per2*$^{-/-}$ and *Per2*$^{+/+}$ mice were analysed. At this advanced age, *Per2* deletion led to a significant increase in total HSC number in bone marrow compared with *Per2*$^{+/+}$ mice (Fig. 1g,j, $P = 0.022$). Interestingly, *Per2* deletion improved the maintenance of Ly-biased HSCs (low expression of CD150: CD150^{lo} CD34^{-} KSL) in ageing mice, whereas the maintenance of My-biased HSCs (high expression of CD150: CD150^{hi} CD34^{-} KSL) was not affected (Fig. 1h–j). *Per2* deletion also improved the maintenance of Ly-biased HSCs in the context of accelerated ageing induced by γ-irradiation (Supplementary Fig. 2A–C).

Per2 is upregulated in haematopoietic cells in response to ageing and DNA damage and contributes to the induction of DNA damage responses

In agreement with previous studies on DNA damage accumulation in mouse and human HSCs during ageing[11,12,28], analyses of DNA damage foci revealed increased numbers of DNA damage foci in HSCs of 16–30-month-old mice compared with 2–3-month-old mice, but no significant impact of *Per2* gene status on these kinetics of DNA damage accumulation (Fig. 2a,b). The induction of DNA damage foci in HSCs in response to γ-irradiation of young mice was also unaffected by the *Per2* gene status (Supplementary Fig. 3A). Together, these data indicated that *Per2* deletion does not affect the sensing of DNA damage or the kinetics of DNA damage accumulation during ageing.

Phosphorylation of replication protein A2 (p-RPA2) is an upstream signal transducer activated by DNA damage in response to replication stress[29,30]. The analysis of serially transplanted HSCs from tertiary recipients (same experiment as depicted in Fig. 1f) revealed a reduced number of nuclear foci of p-RPA2 in HSCs derived from *Per2*$^{-/-}$ donors compared with *Per2*$^{+/+}$ donor mice (Fig. 2c,d). Similarly, *Per2* deletion delayed the induction of p-RPA2 foci in the nuclei of freshly isolated HSCs of 2-month-old mice that were exposed to hydroxyurea—a potent inducer of replication stress[31]—in primary culture (Fig. 2e). Together, these results indicated that *Per2* deletion ameliorates the induction of DNA replication stress signalling in haematopoietic stem and progenitor cells.

Upstream DNA damage responses include the activation of ATM/CHK2 and ATR/CHK1 kinases leading to the activation of downstream signalling cascades. Western blot analysis revealed that *Per2* deletion impaired the induction of upstream and downstream DNA damage signals in haematopoietic bone marrow cells (Lin^{-} cells) of 2–3-month-old mice in response to γ-irradiation (Fig. 2f–h). This included the induction of p53-dependent apoptosis. Specifically, p53 phosphorylation, p53 target gene induction (p21, BAX and PUMA), cleavage of CASP3 (a downstream inducer of apoptosis) and the inhibition of BCL2 (a negative regulator of apoptosis) were blunted in Lin^{-} cells of *Per2*-deficient mice compared with wild-type mice (Fig. 2h). Functional studies on freshly isolated haematopoietic stem and progenitor cells (KSL cells) revealed that γ-irradiation-induced apoptosis was partially rescued by *Per2* deletion (Supplementary Fig. 3B). Together, these data indicated that *Per2* contributes to the induction of DNA damage signals and apoptosis in haematopoietic stem and progenitor cells.

To determine whether *Per2* itself was regulated in response to DNA damage, *Per2* messenger RNA and PER2 protein levels were determined in response to γ-irradiation in 2–3-month-old mice. In response to γ-irradiation, a significant induction of *Per2* mRNA was

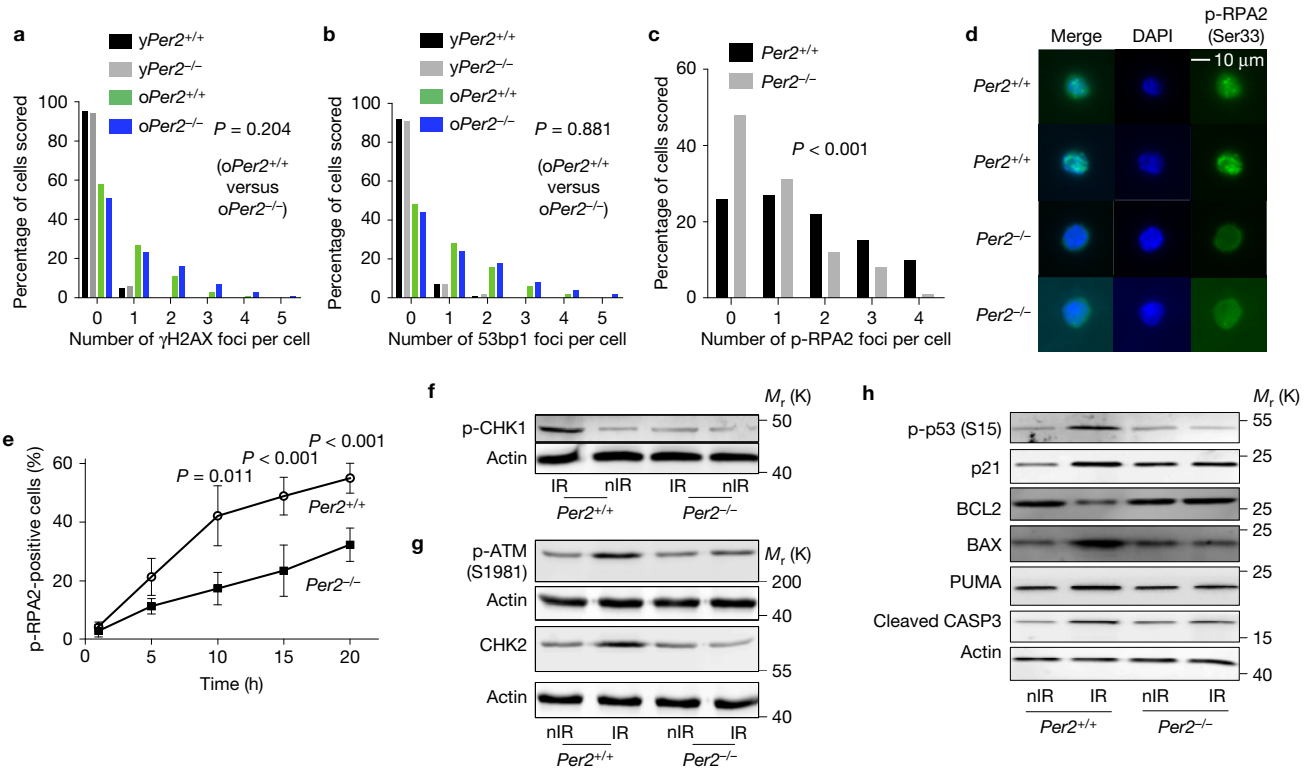

Figure 2 *Per2* contributes to the activation of DNA damage signalling and *p53*-dependent apoptosis in haematopoietic cells in response to DNA damage. (**a**,**b**) DNA damage foci were determined by immunofluorescence staining of freshly isolated HSCs (CD34$^-$ KSL) from 2–3-month-old mice (young (y)) and 16–30-month-old mice (old (o)) of the indicated genotypes. The histograms depict the percentage of purified HSCs showing the indicated number of γH2AX-positive foci (**a**) and 53bp1-positive foci (**b**) per cell. Representative data derived from 200 analysed cells for 1 out of 8 mice per genotype are shown. χ^2 test was used to calculate *P* values. (**c**,**d**) Total bone marrow cells of 2-month-old *Per2*$^{-/-}$ mice or age-matched wild-type mice were transplanted for three rounds into lethally irradiated recipients (the same experiment as in Fig. 1f). Three months after the third round of transplantation, HSCs (CD34$^-$ KSL) were purified and stained for the formation of phosphorylated-RPA2 (Ser33) foci. (**c**) The histogram depicts the percentage of purified HSCs from *Per2*$^{-/-}$ and *Per2*$^{+/+}$ mice showing the indicated number of p-RPA2 foci per cell. Representative data derived from 200 analysed cells for 1 out of 5 mice per genotype are shown. χ^2 test was used to generate *P* values. (**d**) Representative photographs of p-RPA2-stained HSCs of the indicated genotypes. (**e**) 500 freshly isolated HSCs from 2-month-old *Per2*$^{-/-}$ mice and *Per2*$^{+/+}$ mice were cultured overnight and then exposed to hydroxyurea (1 mM) followed by immunofluorescence staining for detection of p-RPA2 foci. The graph shows the percentage of p-RPA2-positive HSCs of mice of the indicated genotypes at the indicated time points after starting the hydroxyurea treatment. $N = 5$ mice per group; values are shown as mean ± s.e.m. Multiple *t*-test was used to calculate *P* values. (**f**–**h**) Western blot analyses of whole-cell lysates from freshly isolated lineage$^-$ bone marrow cells extracted from 2-month-old *Per2*$^{+/+}$ mice and age-matched *Per2*$^{-/-}$ mice that were non-irradiated (nIR) or kept for 6 h after 6 Gy γ-irradiation (IR). Representative western blots using pooled material of 4 mice per group probed for phosphorylated-CHK1 (**f**), phosphorylated-ATM and CHK2 (**g**), and phosphorylated-p53 (**h**), as well as total protein of p21, BCL2, BAX, PUMA and cleaved CASP3. Each assay was repeated three times. Unprocessed photographs of larger sections of the original scans of blots are shown in Supplementary Fig. 6.

seen in HSCs and this induction was p53 independent (Fig. 3a). An induction of PER2 in response to DNA damage was also seen at the protein level in lineage-negative haematopoietic stem and progenitor cells, which was independent of both *p53* and *Atm* gene status (Fig. 3b,c). Of note, the upregulation of *Per2* mRNA in response to DNA damage was more pronounced in Ly-biased HSCs compared with My-biased HSCs (Fig. 3d).

As ageing is associated with increases in DNA damage[11] (Fig. 2a,b) and replication stress[15,16] in HSCs, we investigated the induction of *Per2* in haematopoietic stem and progenitor cells of ageing mice. Immunofluorescence staining revealed an upregulation of the PER2 protein in HSCs of aged WT mice compared with young WT mice, appearing as intra-nuclear PER2 foci (Fig. 3e,f). The PER2 protein was also induced in haematopoietic stem and progenitor cells from 30-month-old WT mice compared with 2-month-old WT mice (Fig. 3g). Also in ageing, *Per2* mRNA increased predominantly in Ly-biased HSCs but not in My-biased HSCs of aged WT mice (Fig. 3h). A premature increase in mRNA expression of *Per2* was detected in HSCs (CD34$^-$ KSL) of 12-month-old G3 *mTerc*$^{-/-}$ mice compared with 2-month-old G3 *mTerc*$^{-/-}$ mice (Fig. 3i).

Together, γ-irradiation, telomere dysfunction and physiological ageing increase *Per2* expression in haematopoietic stem and progenitor cells, which, in the HSC pool, is more pronounced in the subpopulation of Ly-biased HSCs compared with My-biased HSCs. To determine the consequences of *Per2* induction on HSC maintenance and function, freshly isolated KSL cells from wild-type mice or *G3 mTerc*$^{-/-}$ were infected with a cDNA of *Per2* or an empty control virus (Supplementary Fig. 1A). Transplantation of infected KSL cells into lethally irradiated recipients demonstrated a strong negative effect of *Per2* overexpression on the repopulation capacity of HSCs derived from either wild-type donor mice or *G3*

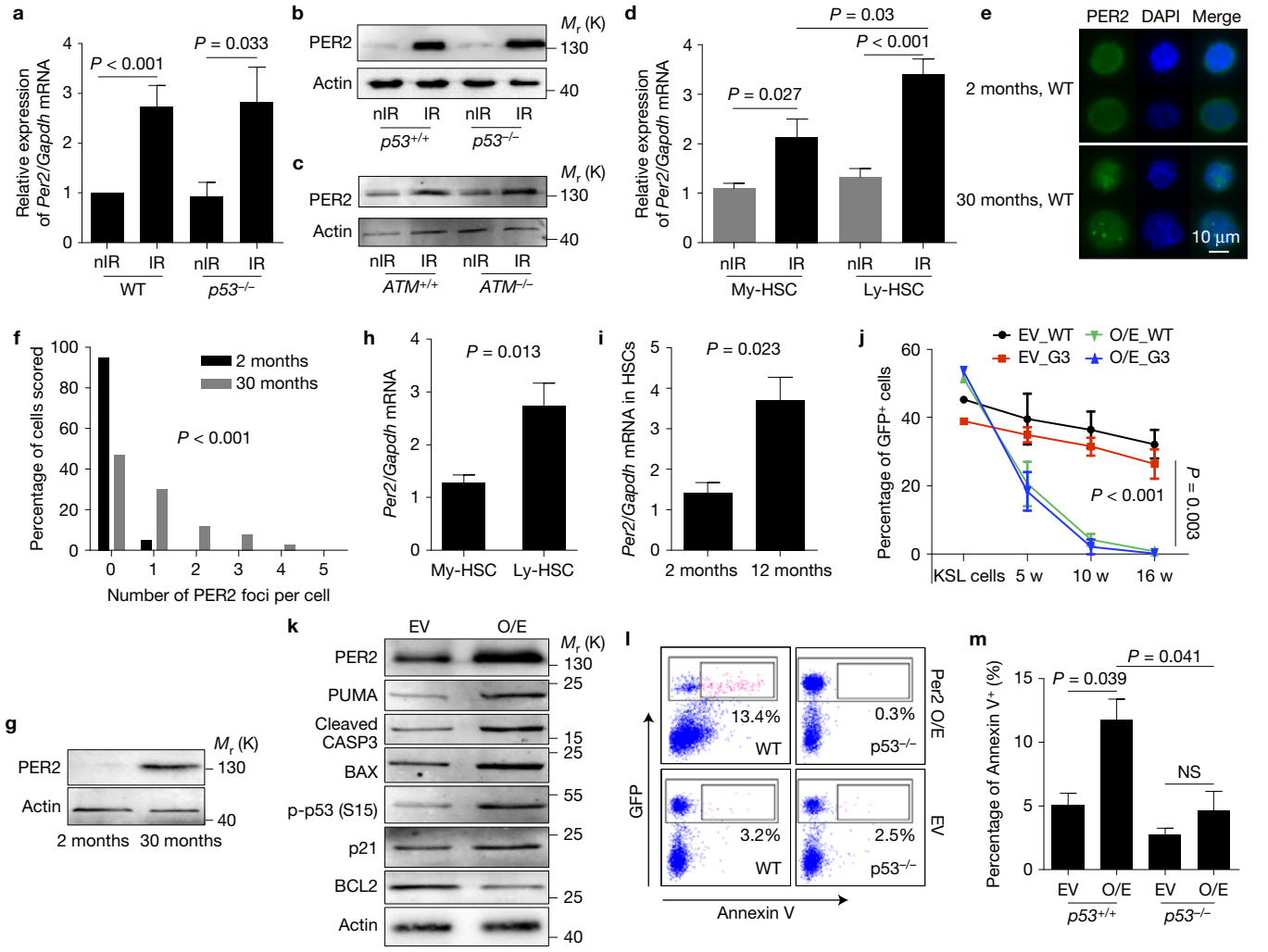

Figure 3 Activation of *Per2* is pronounced in Ly-biased HSCs and contributes to apoptosis induction in haematopoietic cells in response to DNA damage. (**a**–**d**) Haematopoietic cells were extracted from 3-month-old mice, 6 h after γ-irradiation (IR, 6 Gy) or without IR exposure (nIR). (**a**) *Per2* mRNA expression in HSCs of 3-month-old *p53*$^{+/+}$ (WT) or *p53*$^{-/-}$ mice. (**b**,**c**) Western blots showing PER2 expression in Lin$^-$ cells in mice of the indicated genotypes. Data represent 1 out of 3 independent experiments. (**d**) *Per2* mRNA expression in Ly-biased and My-biased HSCs of wild-type mice. (**e**,**f**) HSCs from 2- and 30-month-old wild-type mice were analysed by immunofluorescence for PER2 expression. (**e**,**f**) Representative photos (**e**) and quantification (**f**) of PER2 foci in HSCs of aged compared with young mice. Representative data derived from 200 analysed cells for 1 out of 5 mice per genotype are shown. χ^2 test was used to generate *P* values. (**g**) Western blot showing PER2 expression in Lin$^-$ cells of 2- and 30-month-old wild-type mice. Data represent 1 out of three independent experiments. (**h**) The histogram shows relative expression of *Per2* mRNA in Ly-biased and My-biased HSCs of aged WT mice (26–30 months old). (**i**) *Per2* mRNA expression in HSCs from 3- and 12-month-old G3 *mTerc*$^{-/-}$ mice. (**a**,**d**,**h**,**i**) $N = 5$ mice per group; values are means ± s.e.m.; multiple *t*-test was used to calculate *P* values. (**j**–**m**) Haematopoietic (Lin$^-$ or KSL) cells from 3-month-old mice were infected with a *Per2* cDNA (O/E) or an empty lentivirus (EV) each co-expressing GFP. (**j**) Transplantation of infected KSL cells from G3 *mTerc*$^{-/-}$ and wild-type mice along with non-infected cells into lethally irradiate recipients. The percentage of GFP$^+$ (virally transduced) cells in peripheral blood at indicated time points after transplantation. $N = 5$ mice per group; values as means ± s.e.m. (**k**) Expression of apoptosis-related genes in infected Lin$^-$ cells, 4 days after infection. Data represent 1 out of 3 independent experiments. (**l**,**m**) Analysis of apoptotic cells in freshly isolated KSL cells from *p53*$^{+/+}$ or *p53*$^{-/-}$ mice, 60 h after viral transduction of the isolated cells with an empty vector (EV) or a *Per2* cDNA-expressing vector (O/E). (**l**,**m**) Representative FACS blots (**l**) and histogram (**m**) of the rate of Annexin V$^+$ cells in the indicated groups. $N = 5$ repeat experiments; values are shown as means ± s.e.m.; multiple *t*-test was used to calculate the *P* values. NS, not significant. Unprocessed photographs of larger sections of the original scans of blots are shown in Supplementary Fig. 6.

mTerc$^{-/-}$ donor mice (Fig. 3j). Western blot analysis depicted a significant induction of p53 phosphorylation and apoptosis signalling in *Per2*-cDNA- versus control virus-infected Lin$^-$ cells from wild-type mice (Fig. 3k). This was accompanied by a significant induction of KSL cell apoptosis, which was p53 dependent (Fig. 3l,m). Together, these results indicated that *Per2* overexpression induces apoptosis and limits the repopulation capacity of HSCs.

Per2 deletion rescues ageing-associated impairments in lymphopoiesis and immune function in ageing mice

The above data indicated that *Per2* deletion improves the maintenance of Ly-biased HSCs in ageing mice (Fig. 1g–i). These data prompted us to investigate the consequences of *Per2* deletion on ageing-associated impairments in lymphopoiesis and immune functions—which is thought to contribute to increased morbidity and mortality during

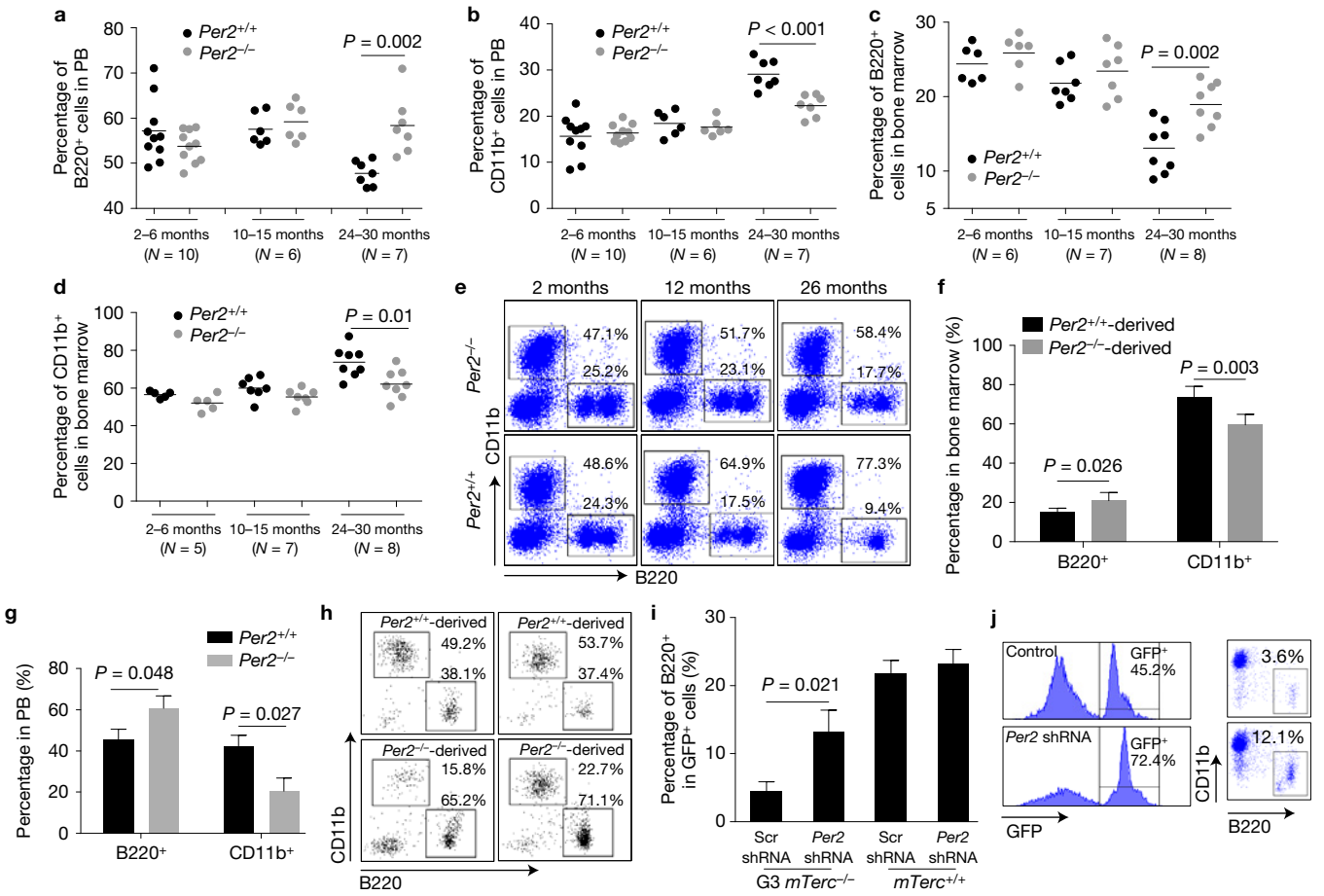

Figure 4 *Per2* deletion rescues myeloid/lymphoid skewing of haematopoiesis in the context of physiological ageing and telomere shortening. (**a**–**d**) The percentage of B220$^+$ cells (**a**,**c**) and CD11b$^+$ cells (**b**,**d**) was determined in peripheral blood (**a**,**b**) and bone marrow (**c**,**d**) of mice of the indicated age and genotype. Dots (*n*) represent individual mice; lines depict mean values; multiple *t*-test was used to calculate *P* values (see also Supplementary Fig. 4A–C). (**e**) Representative FACS plots showing the percentage of B220$^+$ and CD11b$^+$ cells in bone marrow of mice of the indicated age and genotype. (**f**–**h**) 100 freshly isolated HSCs from 20-month-old *Per2*$^{-/-}$ mice (CD45.2) were mixed with 100 freshly isolated HSCs from age-matched wild-type mice (CD45.1) and the mixture was transplanted into sub-lethally (8 Gy) irradiated recipients (CD45.1/.2). Recipients were analysed 5 months after transplantation. (**f**,**g**) Percentage of B220$^+$ and CD11b$^+$ donor-derived cells in bone marrow (**f**) and in peripheral blood (**g**). $N = 5$ mice per group; values are means ± s.e.m.; multiple *t*-test was used to calculate *P* values. (**h**) Representative FACS plots on B220$^+$ and CD11b$^+$ cells in peripheral blood of the recipients. (**i**,**j**) Freshly isolated KSL cells from 2- to 3-month-old *mTerc*$^{+/+}$ mice and G3 *mTerc*$^{-/-}$ mice were infected with scrambled or *Per2*-targeting shRNAs. Infected cells were transplanted along with non-infected cells into lethally irradiated recipients. (**i**) The percentage of B220$^+$ cells in GFP$^+$ (lentiviral targeted) bone marrow cells was evaluated 3 months after transplantation. $N = 5$ mice per group; values are mean ± s.e.m.; multiple *t*-test was used to calculate *P* values. (**j**) Representative FACS plots showing GFP$^+$ cells in total bone marrow (left) and B220$^+$ and CD11b$^+$ cells within the fraction of GFP$^+$ bone marrow cells (right) in 1 out of 5 repeat experiments.

ageing[32]. Interestingly, *Per2* deletion significantly ameliorated ageing-associated skewing in myelo-/lymphopoiesis characterized by a decrease in B220$^+$ B cells and an increase in CD11b$^+$ myeloid cells in peripheral blood and bone marrow of 24-month-old mice (Fig. 4a–e). Similarly, *Per2* deletion rescued premature skewing in myelo-/lymphopoiesis occurring in 15-month-old mice that were exposed to a single, sub-lethal dose of irradiation (4 Gy) at three months of age (Supplementary Fig. 4A–C). To evaluate whether this rescue was at the cell-intrinsic level (not dependent on a *Per2*$^{-/-}$ tissue environment), 100 highly purified HSCs (CD34$^-$ KSL) from 20-month-old *Per2*$^{-/-}$ mice (CD45.2) and *Per2*$^{+/+}$ (CD45.1) donor mice were mixed and transplanted into sub-lethally (8 Gy) irradiated 2-month-old recipient mice (CD45.1/CD45.2). Five months after transplantation, the percentage of B lymphocytes (B220$^+$) and myeloid cells (CD11b$^+$) was determined in the fraction of donor-HSC-derived peripheral blood cells. This analysis confirmed that *Per2* deletion improves the cell-intrinsic potential of HSCs from ageing mice to generate B lymphocytes in bone marrow and peripheral blood (Fig. 4f–h).

Telomere dysfunction was shown to aggravate ageing-associated skewing in lympho-/myelopoiesis by induction of stem-cell-intrinsic checkpoints[18] and alterations in the blood circulatory environment of ageing G3 *mTerc*$^{-/-}$ mice[33,34]. To test whether *Per2* represents an HSC-intrinsic factor contributing to skewing in lympho-/myelopoiesis in response to telomere dysfunction, freshly isolated haematopoietic stem and progenitor cells (KSL cells) from 3-month-old G3 *mTerc*$^{-/-}$ mice or *mTerc*$^{+/+}$ mice were infected with an shRNA against *Per2* or a scrambled shRNA control

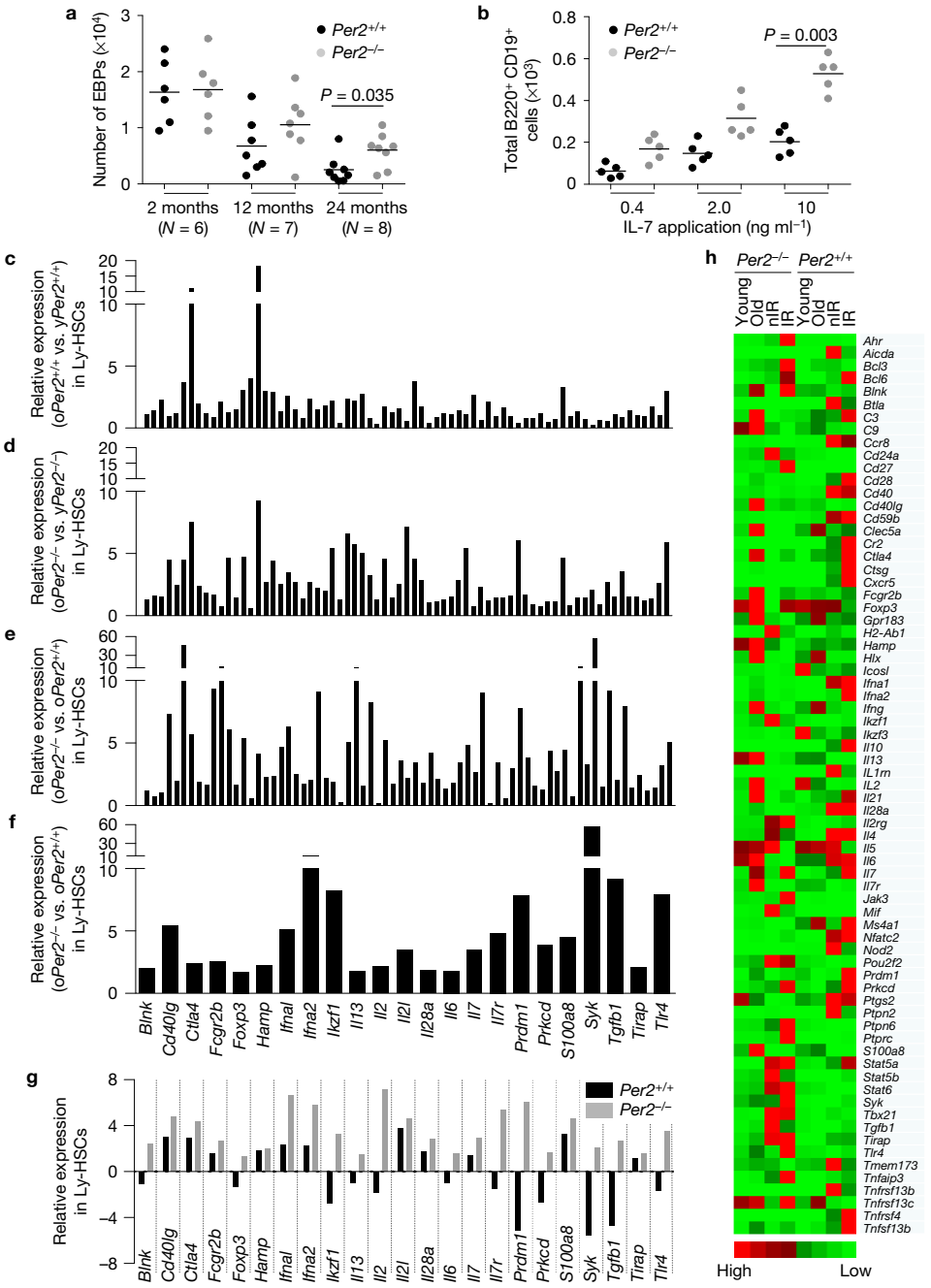

Figure 5 *Per2* deletion improves lymphopoiesis at the stem and progenitor cell level in ageing mice. (**a**) The dot plot shows the number of early B cell progenitors (EBPs, lineage IL7Ra$^+$AA4$^+$ Sca-1^{low}) in bone marrow of mice of the indicated age and genotype. Dots (*n*) represent individual mice; lines depict mean values; multiple *t*-test was used to calculate *P* values. Note the partial rescue in EBP numbers in 24-month-old *Per2*$^{-/-}$ compared with *Per2*$^{+/+}$ mice. (**b**) 1,000 freshly purified EBPs from 30-month-old *Per2*$^{-/-}$ and *Per2*$^{+/+}$ mice were cultured with addition of the indicated concentrations of IL-7. The total number of B220$^+$CD19$^+$ cells was determined after 4-day culture. $N = 5$ mice per group; lines depict mean values; multiple *t*-test was used to calculate *P* values (see also Supplementary Fig. 5A). (**c**–**h**) 50 freshly isolated Ly-biased HSCs from 2-month-old and 24-month-old *Per2*$^{-/-}$ mice or *Per2*$^{+/+}$ mice were profiled by NanoString technology to evaluate the expression of 71 lymphopoiesis-/lymphocyte activation-related genes. 3–5 mice per genotype and age group were pooled: *Per2*$^{-/-}$ young ($n = 3$), old ($n = 3$), non-irradiated (nIR) ($n = 3$), irradiated (IR) ($n = 3$); *Per2*$^{+/+}$ young ($n = 3$), old ($n = 3$), non-irradiated (nIR) ($n = 5$), irradiated (IR) ($n = 5$). Measurements were replicated twice; values are shown as means. (**c**–**e**) The histograms depict relative changes in the expression of the entire gene in Ly-biased HSCs of 24-month-old ('old', o) *Per2*$^{+/+}$ mice compared with 2-month-old ('young', y) *Per2*$^{+/+}$ mice (**c**), Ly-biased HSCs of o*Per2*$^{-/-}$ mice compared with y*Per2*$^{-/-}$ mice (**d**), and Ly-biased HSCs of o*Per2*$^{-/-}$ mice compared with o*Per2*$^{+/+}$ mice (**e**). (**f**) The histogram depicts the relative expression of 23 lymphopoiesis-regulating genes that show an upregulation (>1.5 fold, selected from **e**) in Ly-biased HSCs of 24-month-old *Per2*$^{-/-}$ compared with age-matched *Per2*$^{+/+}$ mice. (**g**) Relative expression of 23 lymphoid genes (the same as in **f**) in Ly-HSCs of 24-month-old *Per2*$^{+/+}$ against 2-month-old *Per2*$^{+/+}$ mice (black bar) and 24-month-old *Per2*$^{-/-}$ against 2-month-old *Per2*$^{-/-}$ mice (grey bar). (**h**) Heat map profile on the relative expression level of 71 lymphopoiesis-/lymphocyte activation-related genes in Ly-biased HSCs of mice of the indicated age, treatment and genetic background. Colours (light red (high) to light green (low)) indicate the range of expression levels of the individual genes at the indicated scaling per row. Expression levels in between rows are not cross-comparable.

vector. The transduced KSL cells were transplanted into lethally irradiated 2-month-old wild-type mice. The percentage of B220$^+$ B lymphocytes was determined three months after transplantation in the compartment of virally transduced, donor-derived cells in the bone marrow of the recipient mice. This analysis revealed that *Per2* knockdown significantly ameliorated telomere-dysfunction-induced HSC-intrinsic impairments in B lymphopoiesis in bone marrow (Fig. 4i,j).

Ageing-associated impairments in lymphopoiesis also occur at the progenitor cell level. Early B lymphocytic progenitors (EBPs: Lin$^-$IL7Ra$^+$AA4$^+$Sca-1^{low}) are strongly diminished in bone marrow of ageing mice[35]. Accordingly, fluorescence-activated cell sorting (FACS) analysis depicted a strong ageing-associated impairment in bone marrow EBPs in ageing wild-type mice, which, however, was partially rescued by *Per2* deletion (Fig. 5a). EBPs continue to differentiate into more mature cells of the B lymphocytic lineage. This process can be stimulated in culture by the addition of interleukin-7 (IL-7). To test the influence of *Per2* gene status on the potential of EBPs to generate B220$^+$ CD19$^+$ B lymphocytes, freshly isolated EBPs from 2- to 3-month-old mice and 30-month-old mice ($n=5$ mice per group) were exposed to increasing concentrations of IL-7 in primary culture. *Per2* deletion significantly improved the potential of EBPs from 30-month-old mice to generate B220$^+$ CD19$^+$ B lymphocytes on IL-7 stimulation in culture (Fig. 5b) but *Per2* gene status did not affect the potential of EBPs from 2- to 3-month-old mice (Supplementary Fig. 5A).

Together, these data indicated that *Per2* deficiency partially rescues ageing-induced impairment in the potential of HSCs and progenitor cells to maintain B lymphopoiesis. To identify possible candidate genes that mediated the beneficial effects of *Per2* deletion on the lymphopoietic potential of ageing HSCs, the mRNA expression of 71 lymphopoiesis-associated genes was analysed in highly purified Ly-biased HSCs from 2- and 24-month-old *Per2*$^{+/+}$ mice and *Per2*$^{-/-}$ mice (Fig. 5c–h). This analysis identified 23 lymphopoiesis-regulating genes that showed an increased expression level (>1.5 fold) in Ly-biased HSCs of aged *Per2*$^{-/-}$ mice compared with *Per2*$^{+/+}$ mice (Fig. 5e–g), including some important positive regulators of lymphocyte development and maturation, such as Blnk, Foxp3, interleukin (IL)-2, IL-6, IL-7 and IL-21, IL-7 receptor (IL-7R), Syk, Ikzf1 (also known as Ikaros), Prdm1, Prkcd and Tlr4 (refs 36–48). Some of these factors were suppressed in Ly-biased HSCs of *Per2*$^{+/+}$ mice during ageing but showed sustained or even elevated expression during ageing of *Per2*$^{-/-}$ mice (Fig. 5g) suggesting a possible involvement of these candidate genes in the improvement of lymphopoiesis in ageing *Per2*-deficient compared with wild-type mice.

To analyse whether *Per2* deletion could also rescue the production of mature, functional, competent B lymphocytes in ageing mice, the expression of E47 (a key regulator of B cell differentiation and function, which is known to decrease during ageing)[49] was determined in freshly isolated B220$^+$ splenic B lymphocytes from 2- and 28-month-old *Per2*$^{+/+}$ mice and *Per2*$^{-/-}$ mice. *Per2* deletion partially rescued the ageing-associated decline of E47 expression in 24-month-old mice but had no effect on E47 expression in B lymphocytes from young mice (Fig. 6a). Immunoglobulin G (IgG), secreted by B lymphocytes, represents the most abundant antibody

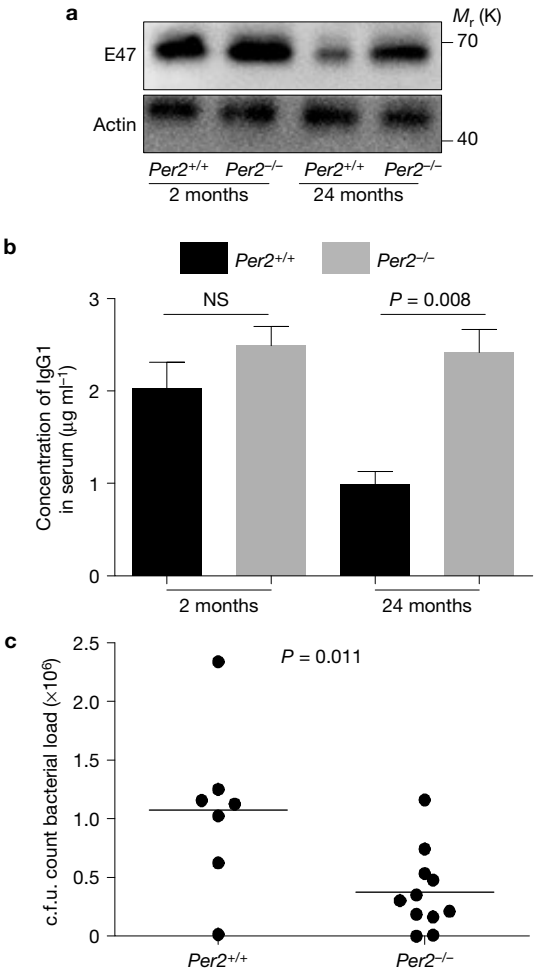

Figure 6 *Per2* deletion rescues immune globulin levels and immune function in aged mice. (**a**) Western blot showing the expression of E47 in B220$^+$ splenocytes of mice of the indicated genotype and age. Data represent one out of three independent experiments. (**b**) The histogram shows the IgG1 level in serum of mice of the indicated genotype and age. $N=5$ mice per group; values are shown as mean ± s.e.m.; multiple *t*-test was used to calculate *P* values. NS, not significant. (**c**) Dot plot showing the bacterial load of the left footpad in 24-month-old mice of the indicated genotype 7 days after subcutaneous inoculation with 1×10^7 colony forming units (c.f.u.) of *S. aureus* 6850 into the left hind footpad. $N=7$ *Per2*$^{+/+}$ mice and $N=11$ *Per2*$^{-/-}$ mice; dots represent individual mice; lines depict mean values; multiple *t*-test was used to calculate *P* values. Unprocessed original scans of blots are shown in Supplementary Fig. 6.

in blood and protects the body from infection. Among the four IgG subclasses, IgG1 is the most abundant (66%) and shows high affinity to bind to the Fc receptor on phagocytic cells[50]. Quantification of IgG1 serum levels revealed a significant elevation of IgG1 in serum of 24-month-old *Per2*$^{-/-}$ mice compared with age-matched *Per2*$^{+/+}$ mice (Fig. 6b). Together, these data indicated that *Per2* deletion improved the production of immune competent lymphocytes at multiple levels in ageing mice. To analyse whether this rescue would indeed result in improved immune function in ageing mice, 24-month-old *Per2*$^{+/+}$ mice and *Per2*$^{-/-}$ mice were challenged by footpad injection of *Staphylococcus aurea* bacteria—a well-established model for chronic infection in mice that leads to activation of innate and adaptive immune responses to clear bacteria infiltration[51]. Of

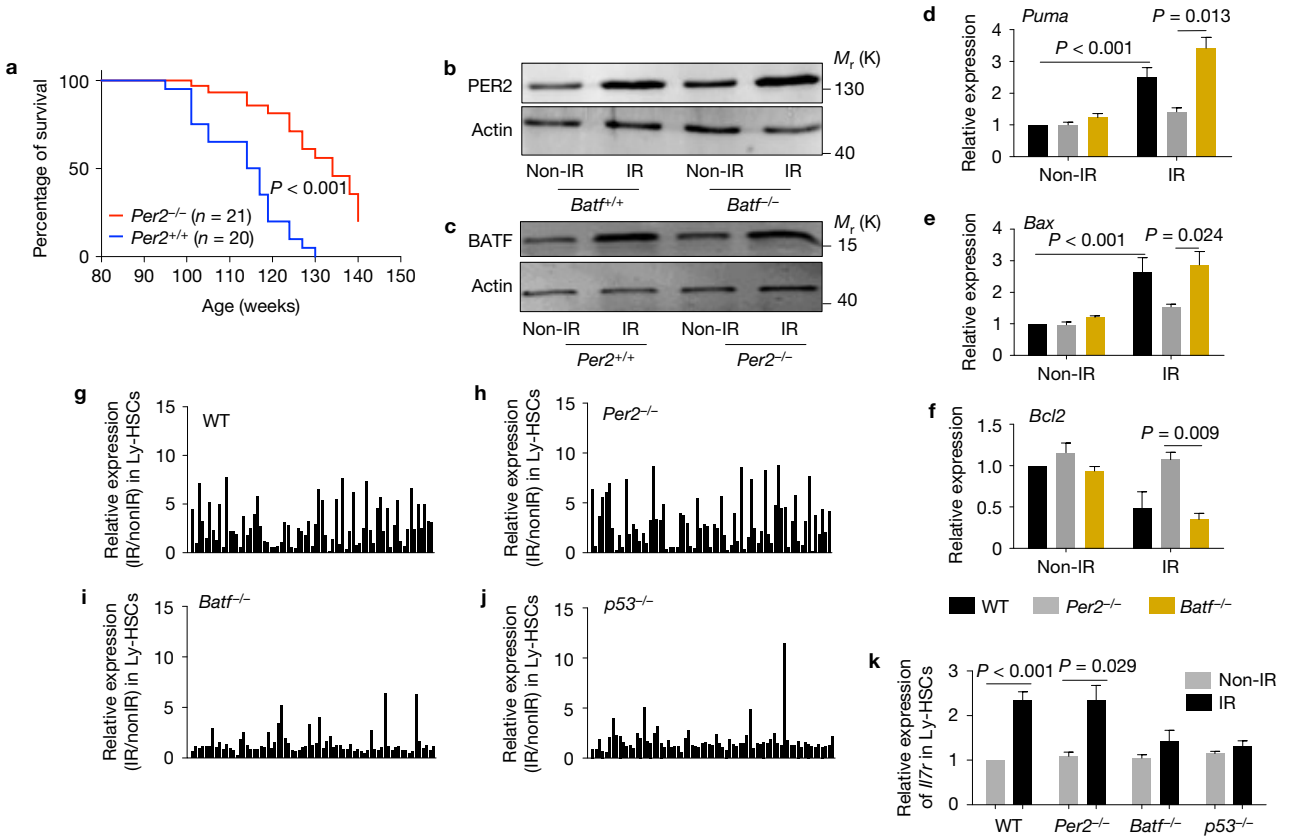

Figure 7 *Per2*$^{-/-}$ mice retain *Batf/p53*-dependent induction of HSC differentiation in response to DNA damage and exhibit an elongated lifespan. (**a**) The Kaplan–Meier plot depicts survival curves for *Per2*$^{-/-}$ ($n=21$) and *Per2*$^{+/+}$ mice ($n=20$). (**b**,**c**) Western blots showing the expression of PER2 (**b**) and BATF (**c**) in lineage-negative bone marrow cells of irradiated (6 Gy, 12 h after IR) and non-irradiated, 2–3-month-old mice of the indicated genotypes. Data represent 1 out of 3 independent experiments. (**d**–**f**) The histograms show the relative expression of the mRNAs of *Puma* (**d**), *Bax* (**e**) and *Bcl2* (**f**) in HSCs from irradiated (6 Gy, 6 h after IR) and non-irradiated, 2–3-month-old wild-type (WT), *Per2*$^{-/-}$ or *Batf*$^{-/-}$ mice. The expression levels of candidate mRNAs were normalized to the expression levels of Gapdh and set to 1 in HSCs of non-irradiated WT mice. $N=5$ mice per group; values are means ± s.e.m.; multiple *t*-test was used to calculate *P* values. (**g**–**j**) The histograms show irradiation-induced changes in the relative mRNA expression of genes associated with B cell differentiation comparing Ly-biased HSCs from irradiated (6 Gy, 6 h after IR) versus non-irradiated, 2–3-month-old wild-type mice of the indicated genotypes: wild-type (WT) (**g**), *Per2*$^{-/-}$ (**h**), *Batf*$^{-/-}$ (**i**) and *p53*$^{-/-}$ (**j**) mice. Pooled samples of 5 mice for WT, *Per2*$^{-/-}$ and *Batf*$^{-/-}$ groups and of 3 mice for *p53*$^{-/-}$ group were measured in 2 replicates, values are shown as means. (**k**) Histogram showing the relative expression changes of interleukin 7 receptor (*Il7r*) in Ly-biased HSCs isolated from irradiated versus non-irradiated mice of the indicated genotypes. $N=5$ mice per group. Values are means ± s.e.m.; multiple *t*-test was used to calculate *P* values. Unprocessed photographs of larger sections of the original scans of blots are shown in Supplementary Fig. 6.

note, the analysis of remaining bacteria in the footpad of mice at 7 days after bacterial infection revealed a significantly improved clearance of bacterial load in the *Per2*$^{-/-}$ cohort compared with the *Per2*$^{+/+}$ cohort (Fig. 6c).

Per2-deficient mice retain *Batf/p53*-dependent DNA damage responses of HSCs and longevity

p53-deficient mice are highly tumour-prone and 100% of the mice develop lymphoma or sarcoma and succumb at an age of 6–8 months[52,53]. The current study showed that *Per2* contributes to the induction of p53 in response to DNA damage in HSCs (Fig. 2h) but *Per2*-deficient mice, in contrast to *p53*-deficient mice, remain tumour-protected (data not shown) and long-lived as observed in our cohort (Fig. 7a) and were previously shown to exhibit only mild increases in spontaneous tumour formation[54]. These data suggest that *Per2*-independent activation of p53 contributes to the suppression of spontaneous tumour formation in *Per2*-deficient mice.

γ-irradiation is known to activate *Batf*—a regulator of AP1 transcription and lymphocyte differentiation—and this leads to differentiation and depletion of HSCs carrying DNA damage[18]. A recent study showed that DNA-damage-induced differentiation restrains the development of haematopoietic malignancies[55]. To test whether *Batf*-dependent induction of DNA damage responses remains intact in *Per2*-deficient HSCs, γ-irradiation-dependent induction of *Batf* and its target genes was determined in haematopoietic stem and progenitor cells. Western blot analysis of Lin$^-$ bone marrow cells revealed that γ-irradiation-induced upregulation of PER2 was independent of *Batf* gene status (Fig. 7b) and vice versa (Fig. 7c). The above data indicated that *Per2* deficiency impaired DNA-damage-induced activation of p53-dependent apoptosis including activation of PUMA and BAX and suppression of BCL2 (Fig. 2h). Of note, these DNA-damage-induced apoptosis signals remained intact in *Batf*-deficient mice (Fig. 7d–f). In contrast, the DNA-damage-dependent induction of lymphoid-differentiation-inducing genes in

HSCs (CD34$^-$ KSL) was highly dependent on *Batf/p53* gene status but largely independent of *Per2* gene status (Figs 7g–j and 5h). In agreement with these results, induction of interleukin 7 receptor mRNA (*Il7r*—a hallmark feature of early lymphoid differentiation) was seen in Ly-biased HSCs in response to DNA damage[18], but this DNA-damage-dependent induction of lymphoid differentiation was completely abolished in Ly-biased HSCs of both $p53^{-/-}$ mice and $Batf^{-/-}$ mice but remained intact in $Per2^{-/-}$ mice (Fig. 7k). Together, these data indicated that DNA damage induces *Per2*- and *Batf*-dependent DNA damage responses in haematopoietic cells and these responses are largely independent from each other.

DISCUSSION

The current study provides experimental evidence that *Per2* represents a central signalling component for the induction of DNA damage responses in haematopoietic stem and progenitor cells. The study shows that *Per2* deletion by itself is sufficient to rescue the maintenance of Ly-biased HSCs, lymphopoiesis and immune functions in ageing mice. These results influence our understanding of molecular mechanisms that contribute to lymphoid/myeloid skewing and functional decline of the ageing haematopoietic system.

Per2 limits self-renewal of Ly-biased HSCs, lymphopoiesis and immune function in ageing mice

This study shows that *Per2* gene status does not affect the ageing-associated increase in My-biased (CD150^{hi}) HSCs but *Per2* deletion leads to an improved maintenance of Ly-biased (CD150^{lo}) HSCs. These data suggest that ageing-associated increases in self-renewal of phenotypic HSCs may in principle affect both Ly-biased (CD150^{lo}) and My-biased (CD150^{hi}) HSCs but the induction of *Per2* limits the ageing-associated increase of phenotypic HSCs in the lymphoid-biased compartment. Previous studies on *Per* genes indicated that *Per1* and *Per2* contribute to the circadian activation of *Atm*/*p53* and *Per2* was shown to mediate apoptosis of thymocytes in response to irradiation[26]. The current study shows that *Per2* itself is upregulated in HSCs in response to ageing and DNA damage. The upregulation of *Per2* under these conditions occurs predominantly in the fraction of Ly-biased HSCs. As overexpression of *Per2* limits the maintenance of HSC function by induction of *p53*-dependent apoptosis (Fig. 3j–m), the selective induction of *Per2* in Ly-biased HSCs is likely to contribute to the reductions in maintenance of Ly-biased HSCs, lymphopoiesis, and in the maintenance of immune functions in ageing mice.

This study also shows that *Per2* deletion ameliorates the induction of DNA replication stress signals in serially transplanted HSCs and in response to hydroxyurea treatment (Fig. 2c–e). DNA replication stress is known to increase in ageing HSCs and to limit HSC function[15,16]. It is tempting to speculate that the here described increase in *Per2* expression in ageing HSCs contributes to this phenomenon by limiting the availability of un-bound timeless, a known factor assisting DNA replication[56]. Accordingly, the deletion of *Per2* could reduce DNA replication stress and the accumulation of DNA damage in ageing HSCs. It is possible that both the rescue in apoptosis signalling and the alleviation of replication stress contribute to the here observed rescue in the maintenance of Ly-biased HSCs in ageing *Per2*-deficient mice compared with wild-type mice without leading to a net increase in DNA damage in ageing HSCs.

Per2-deficient mice retain *Batf*-dependent DNA damage responses and a long cancer-free lifespan

This study showed that the homozygous deletion of *Per2* was associated with no detectable increases in tumour formation (data not shown) whereas a previous study revealed mild increases in the rate of spontaneous cancers in ageing *Per2*-deficient mice[26]. As both studies used pure C57BL/6J mice, possible explanations for differences in the rate of spontaneous cancer may include differences in the mouse cohorts in terms of the pathogen status and/or the gut microbiome—known factors to influence cancer rates also in a genotype-specific manner. It is possible that *Per2* and *Batf* represent alternative routes of p53 activation and HSC depletion in response to DNA damage and these pathways function independent of each other. According to this hypothesis, DNA-damage-induced *Batf/p53*-dependent stem cell differentiation may contribute to the maintenance of tumour suppression in *Per2*-deficient mice. Interestingly, *Per2* mutations were identified as the cause of a subset of familial advanced sleep phase syndromes in human[57]. It is unknown whether these patients show increases in cancer risk or improved immune functions at advanced age.

Together, the findings of the current study provide experimental evidence that *Per2*-dependent DNA damage responses contribute to the decrease in the maintenance of Ly-biased HSCs, lymphopoiesis and immune functions in ageing mice but are dispensable for *Batf/p53* induction of HSC differentiation in response to DNA damage. □

METHODS

Methods and any associated references are available in the online version of the paper.

Note: Supplementary Information is available in the online version of the paper

ACKNOWLEDGEMENTS

This work was supported by the European Union (advanced ERC grant to K.L.R., grant 323136—StemCellGerontoGenes), within the e:Med program (HaematoOpt) of the German Federal Ministry of Education and Research (BMBF), the German Research Foundation (DFG—RU745-10), the Baden-Württemberg-Stiftung (P1301029), the Leibniz association, and the State of Thuringia (FZ-12001-514). We thank Z.-Q. Wang from the Leibniz Institute on Aging for supplying ATM-deficient mice.

AUTHOR CONTRIBUTIONS

J.W. performed most of the experiments; Y.M. performed FACS analysis and wrote the manuscript; B.H. performed ELISA measurements; B.L. and S.N. performed the food pad assay; and K.L.R. designed and supervised the project, and wrote the manuscript.

COMPETING FINANCIAL INTERESTS

The authors declare no competing financial interests.

Published online at http://dx.doi.org/10.1038/ncb3342
Reprints and permissions information is available online at www.nature.com/reprints

1. Rossi, D. J. *et al.* Cell intrinsic alterations underlie hematopoietic stem cell aging. *Proc. Natl Acad. Sci. USA* **28,** 9194–9199 (2005).
2. Geiger, H., Rennebeck, G. & Van Zant, G. Regulation of hematopoietic stem cell aging *in vivo* by a distinct genetic element. *Proc. Natl Acad. Sci. USA* **102,** 5102–5107 (2005).
3. Morrison, S. J., Wandycz, A. M., Akashi, K., Globerson, A. & Weissman, I. L. The aging of hematopoietic stem cells. *Nat. Med.* **2,** 1011–1016 (1996).
4. Sudo, K., Ema, H., Morita, Y. & Nakauchi, H. Age-associated characteristics of murine hematopoietic stem cells. *J. Exp. Med.* **192,** 1273–1280 (2000).
5. Wang, J. W., Geiger, H. & Rudolph, K. L. Immunoaging induced by hematopoietic stem cell aging. *Curr. Opin. Immunol.* **23,** 532–536 (2011).
6. Gazit, R., Weissman, I. L. & Rossi, D. J. Hematopoietic stem cells and the aging hematopoietic system. *Semin. Hematol.* **45,** 218–224 (2008).
7. Linton, P. J. & Dorshkind, K. Age-related changes in lymphocyte development and function. *Nat. Immunol.* **5,** 133–139 (2004).

8. Cho, R. H., Sieburg, H. B. & Muller-Sieburg, C. E. A new mechanism for the aging of hematopoietic stem cells: aging changes the clonal composition of the stem cell compartment but not individual stem cells. *Blood* **111,** 5553–5561 (2008).
9. Beerman, I. *et al.* Functionally distinct hematopoietic stem cells modulate hematopoietic lineage potential during aging by a mechanism of clonal expansion. *Proc. Natl Acad. Sci. USA* **107,** 5465–5470 (2010).
10. Pang, W. W. *et al.* Human bone marrow hematopoietic stem cells are increased in frequency and myeloid-biased with age. *Proc. Natl Acad. Sci. USA* **108,** 20012–20017 (2011).
11. Rossi, D. J. *et al.* Deficiencies in DNA damage repair limit the function of haematopoietic stem cells with age. *Nature* **447,** 725–729 (2007).
12. Rübe, C. E. *et al.* Accumulation of DNA damage in hematopoietic stem and progenitor cells during human aging. *PLoS ONE* **6,** e17487 (2011).
13. Ito, K. *et al.* Reactive oxygen species act through p38 MAPK to limit the lifespan of hematopoietic stem cells. *Nat. Med.* **12,** 446–451 (2006).
14. Ito, K. *et al.* Regulation of oxidative stress by ATM is required for self-renewal of haematopoietic stem cells. *Nature* **431,** 997–1002 (2004).
15. Flach, J. *et al.* Replication stress is a potent driver of functional decline in ageing haematopoietic stem cells. *Nature* **512,** 198–202 (2014).
16. Walter, D. *et al.* Exit from dormancy provokes DNA-damage-induced attrition in haematopoietic stem cells. *Nature* **520,** 549–552 (2015).
17. Choudhury, A. R. *et al.* Cdkn1a deletion improves stem cell function and lifespan of mice with dysfunctional telomeres without accelerating cancer formation. *Nat. Genet.* **39,** 99–105 (2007).
18. Wang, J. W. *et al.* A differentiation checkpoint limits hematopoietic stem cell self-renewal in response to DNA damage. *Cell* **148,** 1001–1014 (2012).
19. Vaziri, H. *et al.* Evidence for a mitotic clock in human hematopoietic stem cells: loss of telomeric DNA with age. *Proc. Natl Acad. Sci. USA* **91,** 9857–9860 (1994).
20. Calado, R. T. & Young, N. S. Telomere maintenance and human bone marrow failure. *Blood* **111,** 4446–4455 (2008).
21. Ohyashiki, J. H. *et al.* Telomere shortening associated with disease evolution patterns in myelodysplastic syndromes. *Cancer Res.* **54,** 3557–3560 (1994).
22. Blasco, M. A. *et al.* Telomere shortening and tumor formation by mouse cells lacking telomerase RNA. *Cell* **91,** 25–34 (1997).
23. Rudolph, K. L. *et al.* Longevity, stress response, and cancer in aging telomerase-deficient mice. *Cell* **96,** 701–712 (1999).
24. Herrera, E. *et al.* Disease states associated with telomerase deficiency appear earlier in mice with short telomeres. *EMBO J.* **18,** 2950–2960 (1999).
25. Chin, L. *et al.* p53 deficiency rescues the adverse effects of telomere loss and cooperates with telomere dysfunction to accelerate carcinogenesis. *Cell* **97,** 527–538 (1999).
26. Fu, L. N. *et al.* The Circadian Gene Period2 plays an important role in tumor suppression and DNA damage response *in vivo*. *Cell* **111,** 41–50 (2002).
27. Beerman, I. *et al.* Proliferation-dependent alterations of the DNA methylation landscape underlie hematopoietic stem cell aging. *Cell Stem Cell* **12,** 413–425 (2013).
28. Beerman, I., Seita, J., Inlay, M. A., Weissman, I. L. & Rossi, D. J. Quiescent hematopoietic stem cells accumulate DNA damage during aging that is repaired upon entry into cell cycle. *Cell Stem Cell* **15,** 37–50 (2014).
29. Lee, Z. & Stephen, J. E. Sensing DNA damage through ATRIP recognition of RPA-ssDNA complexes. *Science* **300,** 1542–1548 (2003).
30. Shao, R. G. *et al.* DNA damage by camptothecin induces phosphorylation of RPA by DNA-dependent protein kinase and dissociates RPA:DNA-PK complexes. *EMBO J.* **18,** 1397–1406 (1999).
31. Vassin, V. M., Anantha, R. W., Sokolova, E., Kanner, S. & Borowiec, J. A. Human RPA phosphorylation by ATR stimulates DNA synthesis and prevents ssDNA accumulation during DNA-replication stress. *J. Cell Sci.* **122,** 4070–4080 (2009).
32. Geiger, H. & Rudolph, K. L. Aging in the lympho-hematopoietic stem cell compartment. *Trends Immunol.* **30,** 360–365 (2009).
33. Ju, Z. *et al.* Telomere dysfunction induces environmental alterations limiting hematopoietic stem cell function and engraftment. *Nat. Med.* **13,** 742–747 (2007).
34. Song, Z. *et al.* Alterations of the systemic environment are the primary cause of impaired B and T lymphopoiesis in telomere-dysfunctional mice. *Blood* **115,** 1481–1489 (2010).
35. Miller, J. P. & Allman, D. The decline in B lymphopoiesis in aged mice reflects loss of very early B-lineage precursors. *J. Immunol.* **171,** 2326–2330 (2003).
36. Minegishi, Y. *et al.* An essential role for BLNK in human B cell development. *Science* **286,** 1954–1957 (1999).
37. Setoguchi, R. *et al.* Homeostatic maintenance of natural Foxp3(+) CD25(+) CD4(+) regulatory T cells by interleukin (IL)-2 and induction of autoimmune disease by IL-2 neutralization. *J. Exp. Med.* **201,** 723–735 (2005).
38. Hori, S. *et al.* Control of regulatory T cell development by the transcription factor Foxp3. *Science* **299,** 1057–1061 (2003).
39. Kaufmann, C. *et al.* A complex network of regulatory elements in Ikaros and their activity during hemo-lymphopoiesis. *EMBO J.* **22,** 2211–2223 (2003).
40. Kopf, M. *et al.* Impaired immune and acute-phase responses in interleukin-6-deficient mice. *Nature* **368,** 339–342 (1994).
41. Puel, A., Ziegler, S. F., Buckley, R. H. & Leonard, W. J. Defective IL7R expression in T(-)B(+)NK(+) severe combined immunodeficiency. *Nat. Genet.* **20,** 394–397 (1998).
42. Nurieva, R. *et al.* Essential autocrine regulation by IL-21 in the generation of inflammatory T cells. *Nature* **448,** 480–483 (2007).
43. Simard, N. *et al.* Analysis of the role of IL-21 in development of murine B cell progenitors in the bone marrow. *J. Immunol.* **186,** 5244–5253 (2011).
44. Limnander, A. *et al.* STIM1, PKC-δ and RasGRP set a threshold for proapoptotic Erk signaling during B cell development. *Nat. Immunol.* **12,** 425–433 (2011).
45. Pasqualucci, L. *et al.* Inactivation of the PRDM1/BLIMP1 gene in diffuse large B cell lymphoma. *J. Exp. Med.* **203,** 311–317 (2006).
46. Alsadeq, A., Hobeika, E., Medgyesi, D., Kläsener, K. & Reth, M. The role of the Syk/Shp-1 kinase-phosphatase equilibrium in B cell development and signaling. *J. Immunol.* **193,** 268–276 (2014).
47. Veldhoen, M., Hocking, R. J., Atkins, C. J., Locksley, R. M. & Stockinger, B. TGFβ in the context of an inflammatory cytokine milieu supports *de novo* differentiation of IL-17-producing T cells. *Immunity* **24,** 179–189 (2006).
48. Hayashi, E. A. *et al.* Role of TLR in B cell development: signaling through TLR4 promotes B cell maturation and is inhibited by TLR2. *J. Immunol.* **174,** 6639–6647 (2005).
49. Frasca, D., Diep, N. D., Riley, R. L. & Blomberg, B. B. Decreased E12/E47 transcription factor activity in the bone marrow as well as in spleen of aged mice. *J. Immunol.* **170,** 2719–2726 (2003).
50. Vidarsson, G., Dekkers, G. & Rispens, T. IgG subclasses and allotypes: from structure to effector functions. *Front Immunol.* **5,** 520 (2014).
51. Nippe, N. *et al.* Subcutaneous infection with *S. aureus* in mice reveals association of resistance with influx of neutrophils and Th2 response. *J. Invest. Dermatol.* **131,** 125–132 (2011).
52. Donehower, L. A. *et al.* Mice deficient for p53 are developmentally normal but susceptible to spontaneous tumours. *Nature* **356,** 215–221 (1992).
53. Jacks, T. *et al.* Tumor spectrum analysis in p53-mutant mice. *Curr. Biol.* **4,** 1–7 (1994).
54. Lee, S., Donehower, L. A., Herron, A. J., Moore, D. D. & Fu, L. Disrupting circadian homeostasis of sympathetic signaling promotes tumor development in mice. *PLoS ONE* **5,** e10995 (2010).
55. Santos, M. A. *et al.* DNA-damage-induced differentiation of leukaemic cells as an anti-cancer barrier. *Nature* **514,** 107–111 (2014).
56. Sangoram, A. M. *et al.* Mammalian circadian autoregulatory loop: a timeless ortholog and mPer1 interact and negatively regulate CLOCK-BMAL1-induced transcription. *Neuron* **21,** 1101–1113 (1998).
57. Toh, K. L. *et al.* An hPer2 phosphorylation site mutation in familial advanced sleep-phase syndrome. *Science* **291,** 1040–1043 (2001).

DOI: 10.1038/ncb3342

METHODS

Mice. All experimental mice were on a C57BL/6J background, maintained in a pathogen-free environment and fed with a standard chow. *mTerc*$^{+/-}$ mice were crossed to generate G1 *mTerc*$^{-/-}$ mice, which were crossed as homozygous knockouts to generate the third generation (G3 *mTerc*$^{-/-}$ mice). *p53*$^{-/-}$ and *Per2*$^{-/}$ mice were purchased from Jackson Lab (Stock number 002101 and 003819). Experiments were conducted according to protocols approved by the state government of Thuringia (Reg. No. 03-006/13) and the state government of Baden-Württemberg (Protocol Number 35/9185.81-3/919). All mice were used for analysis regardless of sex.

Plasmid. All shRNAs (Supplementary Table 1) were purchased from Open Biosystems in the pSM2 backbone and the shRNA cassettes were shuttled into SF-LV-shRNA-EGFP, a self-modified lentiviral vector for shRNA expression[18]. The cDNA of mouse *Per2* was purchased from Addgene (catalogue No. 16204), amplified by PCR and cloned into SF-LV-cDNA-EGFP vector, a self-modified lentiviral vector for cDNA expression.

Western blot. Whole-cell extracts were obtained in RIPA buffer and subjected to 12% SDS–PAGE using antibodies against BATF (1:1,000, Abnova, H00010538-M01), PER2 (1:500, BD Transduction, 611138 and Millipore, AB2202), p-p53 (S15) (1:1,000, Cell Signaling, 9284), BCL2 (1:500, Millipore, 04-436), PUMA (1:1,000, Millipore, AB10418), p21 (1:1,000, Santa Cruz, sc-6246), cleaved CASP3 (1:500, Cell Signaling, 9661), β-actin (1:10,000, Sigma, A2066), E47 (BD Pharmingen, 54077), p-CHK1 (Ser345) (Cell Signaling, catalogue No. 2348, 1:1,000), CHK2 (Calbiochem, catalogue No. PC483, 1:500) and p-ATM (S1981) (Cell Signaling, catalogue No. 4526S, 1:500). Loading and transfer quality of western blots was controlled by Ponceau staining. Proteins recognized by the antibodies were detected with an Odyssey infrared imaging system (LI-COR) using IRDye680RD- or IRDye800CW-coupled secondary antibodies.

Cells and virus production. Lenti-X cells (Clontech, catalogue No. 632180) were cultured in Dulbecco's modified Eagle's medium (DMEM) supplemented with 10% fetal bovine serum and 1% penicillin/streptomycin. Lentivirus was packaged by the plasmids psPAX2 (catalogue No. 36052) and pMD2.G (catalogue No. 12259), which were purchased from Addgene. For lentivirus production, 2×10^6 Lenti-X cells were plated in 10 ml media in a 10 cm tissue culture plate and incubated at 37 °C, in a 5% CO_2 incubator overnight. Cells were transfected by the calcium phosphate method. Five hundred microlitres of 2xHBS (pH 7.12), 12 μg lentiviral shRNA plasmid, 10 μg psPAX2 plasmid and 3 μg pMD2.G plasmid were mixed in a 15 ml tube by vortex for two seconds, and 60 μl 2.5 M $CaCl_2$ solution was added, drop-wise, into the mixture. The mixture was incubated at room temperature for 20 min and gently added into Lenti-X cells, drop-wise. The culture plate was swirled to disperse the mixture evenly. Cells were incubated at 37 °C, in 5% CO_2. After 12 h, the medium was changed. Viral supernatant was collected 36 h after changing the medium.

Lentivirus concentration and titration. Media collected from Lenti-X cells were centrifuged at 800*g* for 10 min to pellet any cells or fragments and filtered with a 0.02 μm filter to remove any tiny fragments. Viruses were pelleted by spinning media at 100,000*g* for 150 min. The viral pellet was resuspended in 50 μl PBS. For titration, 2×10^5 lineage-negative bone marrow cells were cultured in 200 μl SFEM medium (Stem Cell Technology, catalogue No. 09655) with 1% penicillin/streptomycin in a 96-well plate (BD FALCON, catalogue No. 351178) for 24 h. Concentrated virus (1 μl, 5 μl or 20 μl) was added into each well, and incubated with the cells for 8–12 h followed by 2 repeat washes. To analyse the cell infection rate, the percentage of GFP-positive cells is analysed 3 days after infection on an aliquot of cells. Transplantations of infected cells can be conducted directly after infection and repeated washes as described.

KSL cell isolation and viral transduction. Total bone marrow cells from mice were c-Kit enriched by magnetic activated cell separation and c-Kit+ cells were immunolabelled by Sca-1 and lineage antibodies. All c-Kit$^+$ Sca-1$^+$ lineage$^-$ (KSL) cells were purified by FACS. KSL cells (2×10^5) were plated in 200 μl SFEM medium (Stem Cell Technology, catalogue No. 09655) with 1% penicillin/streptomycin, 20 μg ml^{-1} mSCF and 20 μg ml^{-1} thrombopoietin in a 96-well plate (BD FALCON, catalogue No. 351178). Lentivirus suspensions were added into KSL cells according to the titration result. After 3-day culture, infected KSL cells were collected and injected into lethally irradiated recipients.

shRNA screening. We constructed a lentiviral library of 988 shRNAs targeting 459 putative tumour suppressor genes based on Pubmed entries in the years 1980–2009. All shRNAs (Supplementary Table 1) were purchased from Open Biosystems in the pSM2 backbone and the shRNA cassettes were shuttled into a self-modified lentiviral vector[18] by MluI/EcoRI sites. Haematopoietic stem and progenitor cells (c-Kit$^+$, Sca-1$^+$, lineage$^-$ = KSL cells) from 3-month-old G3 *mTerc*$^{-/-}$ mice with critically short telomeres and from age-matched *mTerc*$^{+/+}$ mice with long-telomere reserves ($n = 20$ donor mice per group, Fig. 1a) were purified and infected by a lentivirus pool of 988 shRNAs. Infection rates were 42–65% in both groups; infected and non-infected cells were transplanted for two rounds into lethally irradiated recipients ($n = 20$ recipients per group for each round of transplantation). Four weeks after secondary transplantation, lineage-marker negative (Lin$^-$) haematopoietic progenitor cells were isolated and submitted to deep sequencing analysis. Most shRNAs (967–985 out of 988) remained detectable in the haematopoietic compartment of both groups of donor mice after two rounds of transplantation (Supplementary Fig. 1C). The prevalence of individual shRNAs was determined in Lin$^-$ cells re-derived after secondary transplantation. To verify candidate genes that were positively selected in haematopoietic cells with dysfunctional telomeres, freshly isolated KSL cells from G3 *mTerc*$^{-/-}$ mice or *mTerc*$^{+/+}$ mice were infected with single shRNAs targeting individual candidate genes. Infection rates were 18–50% (as determined by co-expression of GFP in lentiviral shRNA-targeted cells). Infected KSL cells were transplanted into lethally irradiated mice along with non-infected cells from the same culture. The chimaerism of lentiviral shRNA-targeted cells was determined in peripheral blood of recipients at 4-week intervals for up to 16 weeks after transplantation. In both cohorts, scrambled-shRNA-infected KSL cells exhibited a mild negative selection possibly owing to mild toxicity of GFP or virus.

Immunofluorescence staining. One thousand HSCs were seeded on glass slides according to a published method[58] and kept at room temperature for one hour in a humid chamber for the cells to settle onto the slides. Cells on slides were then fixed with 4% PFA for 10 min at room temperature. After washing the cells with PBS twice, the cells were permeabilized with 30 μl 0.5% Triton X-100 for 20 min. Blocking was performed with 30 μl goat serum at room temperature for one hour. Then, the cells were incubated with 30 μl primary antibodies for one hour at room temperature: anti-gH2AX (Millipore, Cat.05-636), anti-53bp1 (Novus Biologicals, Cat. NB100-304), anti-phosphorylated-RPA2 (1:100, EMD Bioscience, Ab-2), anti-Per2 (1:500, BD Transduction, catalogue No. 611138 or Millipore, AB2202). Cells were washed with PBS twice and incubated with 20 μl secondary antibodies with a fluorescent dye for one hour at room temperature in a humid chamber. After washing with PBS twice, stained cells were applied with 10 μl Vectashield mounting medium containing 1.5 mg ml^{-1} of DAPI and a coverslip. Cells with foci were detected under a fluorescence microscope. Two hundred cells were counted for each staining.

Apoptosis analysis. Collected cells were centrifuged and resuspended in 100 μl binding buffer. Cells were then stained with 5 μl Annexin V–APC (BioLegend, catalogue No. 640920) at room temperature in the dark for 15 min. An additional 400 μl binding buffer and propidium iodide were added into the cell suspension. Cells were analysed on a LSRFortessa.

Footpad assay. Mice (24 month old) were inoculated subcutaneously with 1×10^7 c.f.u. of *S. aureus* 6850 into the left hind footpad. The animals were monitored every day and killed by cervical dislocation at day 7. Footpad tissues were homogenized in PBS and plated after serial dilutions on blood agar to determine bacterial loads. Colonies were counted after incubation overnight at 37 °C.

shRNA recovery. Genomic DNA was isolated from Lin$^-$ bone marrow cells (Gentra Puregene Blood Kit, QIAGEN) and the integrated proviral sequences were amplified with primers flanking the mir30 cassette[18].

Limited cell number NanoString. nCounter GX Mouse Immunology V1 Kit was developed by the NanoString R&D team. Targeted genes were amplified from 50 Ly-biased HSCs freshly isolated according to the manufacturer's standard protocol. Fifty per cent of amplified cDNA was loaded to a digital analyser for gene expression quantification and raw data were analysed by using nSolver.

Quantitative real-time PCR. Total RNA was isolated from freshly isolated HSCs by using the MagMAX 96 total RNA isolation Kit (Ambion) according to the manufacturer's protocol. Quantitative real-time PCR was performed with an ABI 7300 Real-Time PCR System (Applied Biosystems) in duplicates from at least three biological samples. The superscript III kit (Invitrogen) was used for cDNA synthesis from total RNA. Supplementary Table 2 depicts primer sets for the detection of single genes. The quantitative PCR was carried out in a volume of 25 μl using the iTaq SYBR Green supermix with Rox (Bio-Rad). Values for mRNA expression were normalized to the expression of Gapdh.

Flow cytometry. For flow cytometric analysis, and sorting, bone marrow cells were collected from mice by crushing bones and single-cell suspensions were stained with antibodies, as previously described[58]. The antibodies used for staining

were: biotinylated anti-mouse Mac-1 Ab (clone M1/70, catalogue No. 101204, Biolegend); 1:400 biotinylated anti-mouse Ter119 antibody (clone Ter119, catalogue No. 116204, Biolegend), 1:200; biotinylated anti-mouse CD8 antibody (clone 53-6.7, catalogue No. 100704, Biolegend), 1:800; biotinylated anti-mouse B220 antibody (clone RA3-6B2, catalogue No. 103204, Biolegend), 1:400; biotinylated anti-mouse CD4 antibody (clone RM4-5, catalogue No. 100508, Biolegend), 1:800; biotinylated anti-mouse CD3 antibody (clone 145-2C11, Cat.100304, Biolegend), 1:800; biotinylated anti-mouse Gr1 antibody (clone RB6-8C5, Cat.108404, Biolegend), 1:200; allophycocyanin-conjugated (APC-) anti-mouse c-Kit antibody (clone 2B8, catalogue No. 17-1171, e-Bioscience), 1:100; Pacific blue-conjugated anti-mouse Sca-1 antibody (clone D7, catalogue No. 122520, Biolegend), 1:100; fluorescein isothiocyanate-conjugated anti-mouse CD34 (clone RAM34, catalogue No. 11-0341, e-Bioscience), 1:30; and phycoerythrin-conjugated (PE-) anti-mouse CD150 antibody (clone TC15-12F12.2, catalogue No. 115903, Biolegend), 1:100. Data acquisition and cell sorting were performed on a FACS LSRII and a FACSAriaII (BD Biosciences). Data were analysed with the FlowJo software.

Competitive transplantation assay followed by irradiation to identify the cell-intrinsic role of *Per2* in selecting haematopoietic stem and progenitor cells in response to DNA damage. One hundred freshly isolated HSCs ($CD34^-$ KSL) from either 2-month-old $Per2^{-/-}$ or $Per2^{+/+}$ mice (both CD45.2) were transplanted along with 1 million competitor cells (total bone marrow from 2-month-old CD45.1 mice) into lethally irradiated recipients ($n = 10$ per group). Four months after transplantation, five mice per group received a second dose (4 Gy) of sub-lethal γ-irradiation and changes in the chimaerism of peripheral blood cells were determined at 2-month intervals.

Serial transplantation assay. One million total bone marrow cells of 2-month-old $Per2^{-/-}$ (CD45.2) or age-matched wild-type (CD45.2) mice were transplanted into lethally irradiated recipients (CD45.1/.2) together with two million competitor bone marrow cells (CD45.1). Three months after transplantation, 5 million total bone marrow cells from the first recipients were re-transplanted into the second recipients. The same procedure was conducted for a third round.

Statistics and reproducibility. GraphPad Prism was used for statistical analyses. Multiple t-test, Gehan–Breslow–Wilcoxon test or χ^2 test were used to generate P values for all data sets and $P < 0.05$ was considered significant. All numerical results are reported as the mean ± s.e.m. and data were represented from three independent experiments with similar results. No statistical method was used to predetermine sample size. The experiments were not randomized, and the investigators were not blinded to allocation during experiments and outcome assessment.

58. Ema, H. *et al.* Adult mouse hematopoietic stem cells: purification and single-cell assays. *Nat. Protoc.* **1,** 2979–2987 (2007).

DOI: 10.1038/ncb3342

nature cell biology

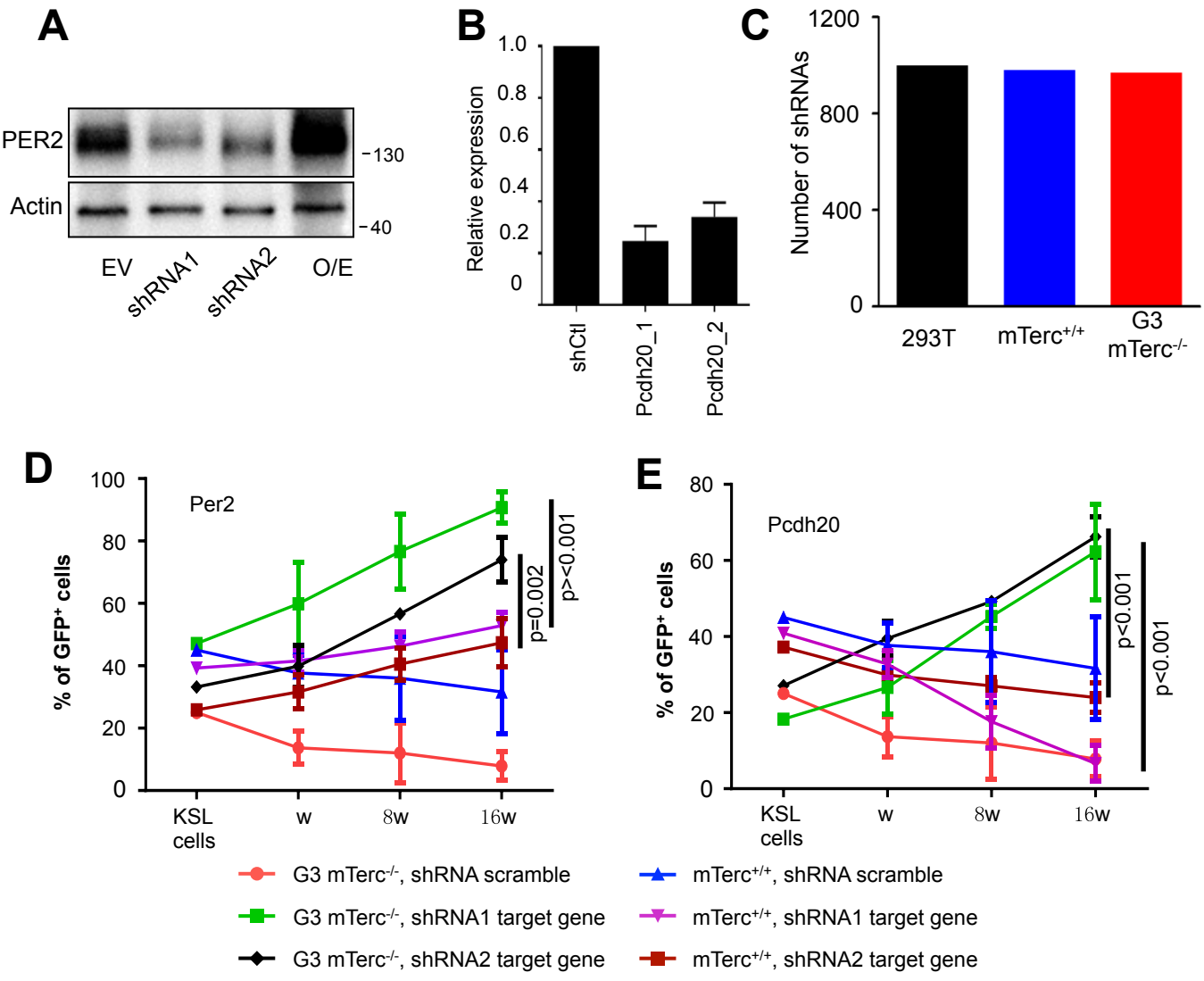

Supplementary Figure 1 Verification of shRNAs of candidate genes A) The representative Western blot shows the efficiency of knockdown (by shRNAs) and over-expression (O/E) of Per2. Cell lysates obtained from lineage$^-$ bone marrow cells that were infected by lentiviral vectors carrying two different shRNA (shRNA1 or shRNA2) targeting *Per2* or Per2-cDNA, or an empty control vector were loaded to detect PER2 protein expression. Data represent 1 out 3 independent experiments. B) The histogram shows the mRNA level of Pcdh20 in lineage$^-$ bone marrow cells of WT mice infected by lentiviruses carrying two different shRNAs against *Pcdh20* or a scramble shRNA control vector. N= 3 repeat experiments, values are means ± SEM. C) The histogram depicts the number of shRNAs detected by deep sequencing in the shRNA plasmid pool as well as in Lin$^-$ cells derived from *mTerc*$^{+/+}$ and G3 *mTerc*$^{-/-}$ donors after two round of transplantation as depicted in Fig. 1A. (D,E) Freshly isolated KSL cells from G3 *mTerc*$^{-/-}$ mice or *mTerc*$^{+/+}$ mice were infected with 2 independent single shRNA constructs targeting (D) *Per2* or (E) *Pcdh20*, or a scrambled shRNA control. Infected cells were transplanted into lethally irradiated mice along with non-infected cells from the same culture. The graphs show the changes in the percentage of infected cells (GFP$^+$) in peripheral blood of primary recipients at indicated time points after transplantation. N= 5 recipients/group, values are means ± SEM, multiple t test was used to calculate p values.

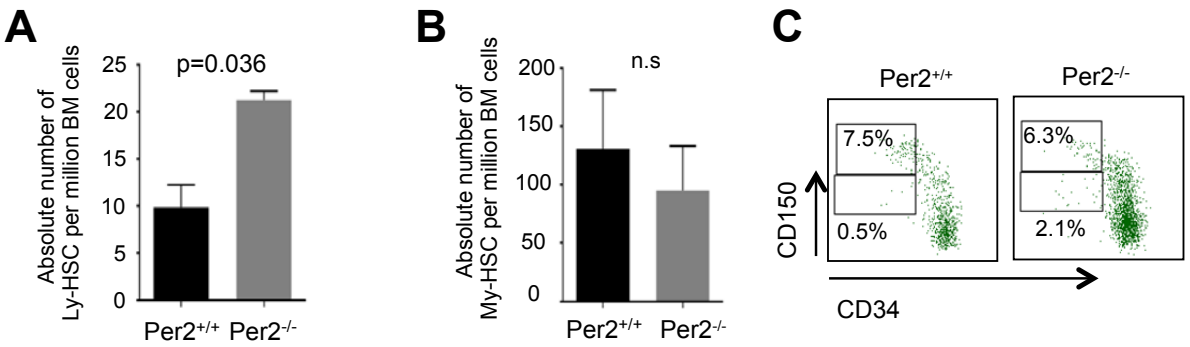

Supplementary Figure 2 *Per2* deletion improves self-renewal of HSCs in response to replicative stress. A-C) Cohorts of 3-month-old *Per2*$^{-/-}$ mice and *Per2*$^{+/+}$ mice were sub-lethally irradiated (4 Gy) to induce premature aging and kept for 1 year. At this time point mice were sacrificed to analyze hematopoietic cells in bone marrow (8 *Per2*$^{+/+}$ mice and 7 *Per2*$^{-/-}$ mice). A,B) The histograms show the absolute number of (A) Ly-biased HSCs (marked by CD150^{lo} CD34^{-} KSL) and (B) My-biased HSCs (marked by CD150^{hi} CD34^{-} KSL), values are shown as mean ± SEM, multiple t test was used to calculate p values. (C) Representative FACS plots showing an increase in Ly-biased HSCs (CD150^{lo}, CD34^{-}) in bone marrow of *Per2*$^{-/-}$ mice *vs.* *Per2*$^{+/+}$ mice. FACS was repeated on biological replicates (8 times for *Per2*$^{+/+}$ mice and 7 times for *Per2*$^{-/-}$ mice).

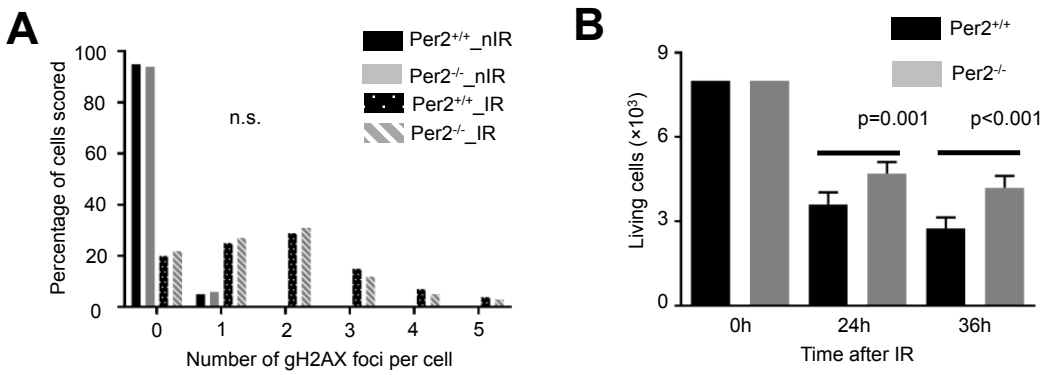

Supplementary Figure 3 *Per2* contributes to the activation of apoptosis signaling in hematopoietic cells in response to DNA damage but not to DNA damage sensing. A) Immunofluorescence staining of γH2AX in freshly isolated HSCs (CD34⁻ LSK) from irradiated (4Gy, 6h after IR) and non-irradiated (nIR), 2-3-month-old *Per2*$^{+/+}$ mice or *Per2*$^{-/-}$ mice. Representative data derived from 200 analyzed cells for 1 out of 5 mice per genotype are shown. Chi-square test was used to generate p values. Note, there is no impact of *Per2* gene status on the induction of γH2AX foci. B) 8000 freshly isolated KSL cells from 2-month-old *Per2*$^{+/+}$ and *Per2*$^{-/-}$ mice were cultured for 12h followed by sub-lethal irradiation (4Gy). The numbers of living cells were counted 24h and 36h after IR by automatic cell counter. This histogram depicts the number of living hematopoietic stem and progenitor cells (KSL) at indicated time points after sub-lethal irradiation (4Gy). N=5 repeat experiments per genotype, values are shown as mean ± SEM and multiple t test was used to calculate p value.

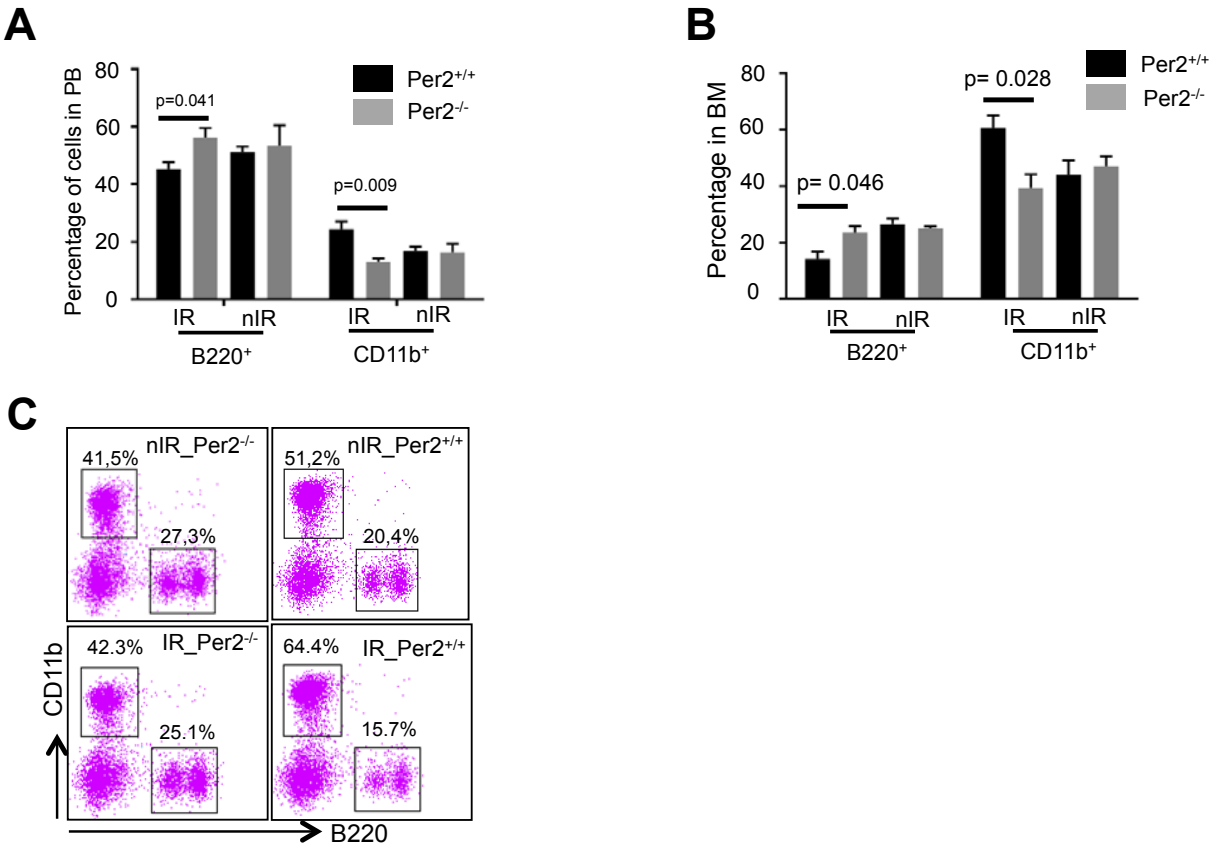

Supplementary Figure 4 *Per2* deletion rescues myeloid/lymphoid skewing in the context of DNA damage. A-C) 3-month-old *Per2*$^{-/-}$ and *Per2*$^{+/+}$ mice were exposed to 4Gy γ-irradiation (IR) or non-irradiated (nIR) and were analyzed one year later (same as in Suppl. Fig. 2). (8 *Per2*$^{+/+}$ mice and 7 *Per2*$^{-/-}$ mice per group), values are shown as mean ± SEM. Multiple t test was used to calculate p value. (A) This histogram shows the percentage of B220^{+} and CD11b^{+} cells in peripheral blood. (B) This histogram shows the percentage of B220^{+} and CD11b^{+} cells in bone marrow (C) Representative FACS plots showing the B220^{+} and CD11b^{+} cells in bone marrow of mice of the indicated genotype and treatment.

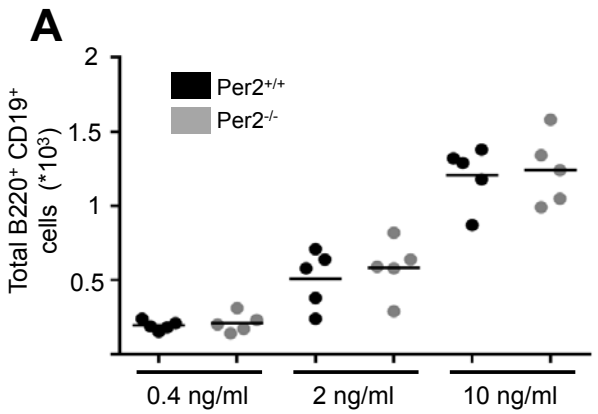

Supplementary Figure 5 *Per2* deletion does not change B-lymphocyte production of stimulated B cell progenitors from young mice. A) 1000 freshly purified EBPs from 2-month-old *Per2*$^{-/-}$ and *Per2*$^{+/+}$ mice were cultured and exposed to IL-7 at the indicated concentrations. FACS analysis determined the total numbers of B220^{+} CD19^{+} cells after 4-day culture. N= 5 mice per group, dots represent individual mice, lines depict mean values. In contrast to the results on EBPs from old mice (Figure 5B), *Per2* gene status does not affect B-lymphocyte production rates of stimulated B-cell progenitors from young mice.

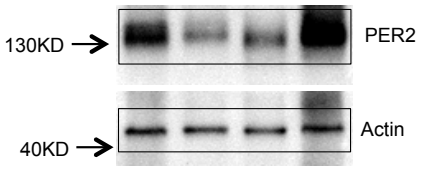

Suppl. Fig. 1A

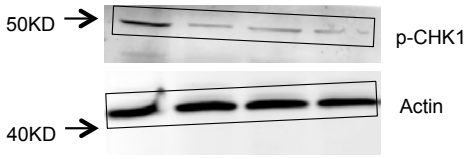

Fig. 2F

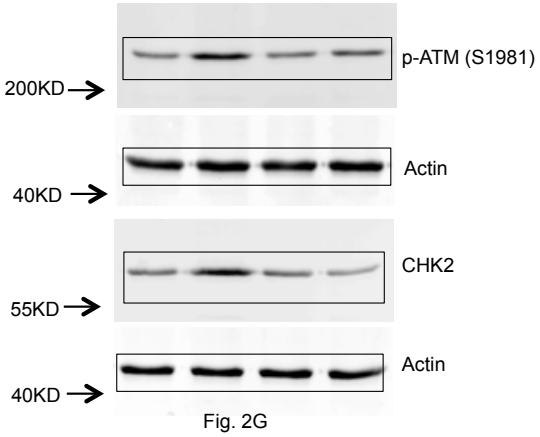

Fig. 2G

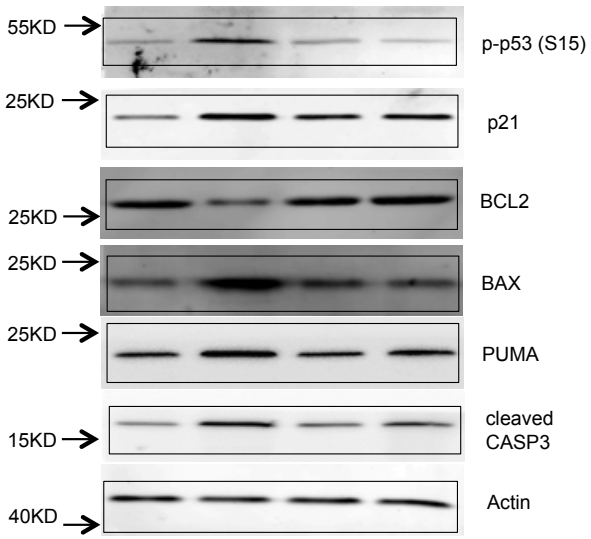

Fig.2H

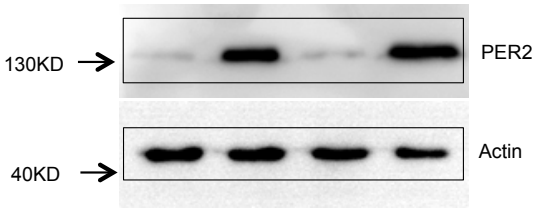

Fig. 3B

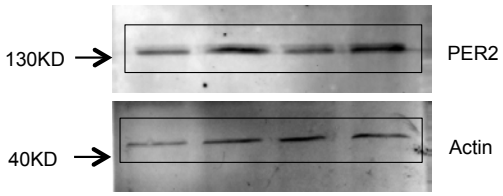

Fig. 3C

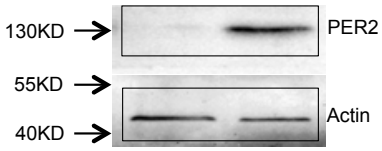

Fig. 3G

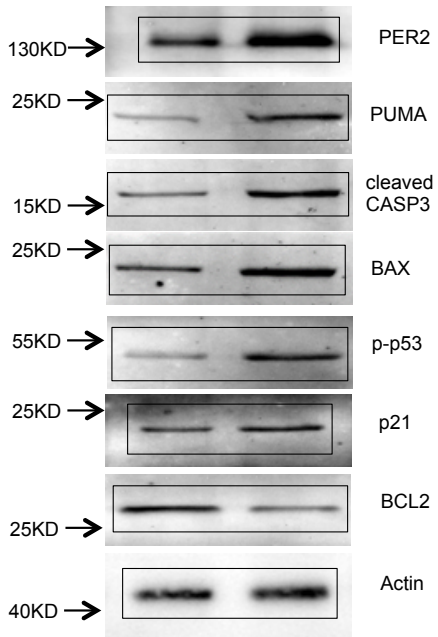

Fig. 3K

Supplementary Figure 6 Unprocessed photographs of bigger sections of the Western blots with size markers corresponding to the indicated Western blots in the main figures. Black squares indicate cutting of Western blots as depicted in main figures. Western blots for detected proteins were run in parallel with Actin control blots with the same loading and running order.

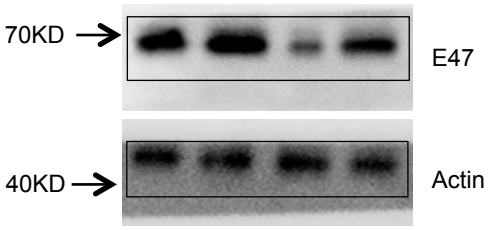

Fig. 6A

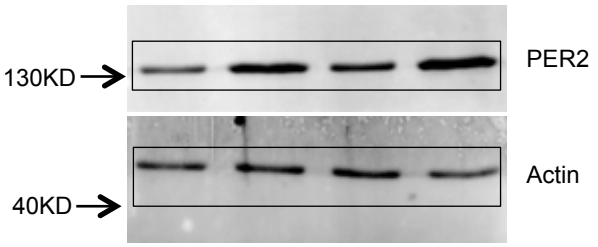

Fig. 7B

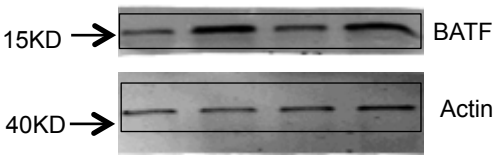

Fig. 7C

Supplementary Figure 6 continued

Supplementary Table Legends

Supplementary Table 1 Details of shRNA screening

Supplementary Table 2 RT-PCR primers